Chromoelectric dipole moments of quarks in MSSM extensions

Amin Aboubrahim, Tarek Ibrahim, Pran Nath, and Anas Zorik

Phys. Rev. D **92**, 035013 — Published 19 August 2015
DOI: 10.1103/PhysRevD.92.035013

Chromoelectric Dipole Moments of Quarks in MSSM Extensions

Amin Aboubrahim[b], Tarek Ibrahim[a*], Pran Nath[c†] and Anas Zorik[d‡]

[a]University of Science and Technology, Zewail City of Science and Technology, 6th of October City, Giza 12588, Egypt[4]

[b]Department of Physics, Faculty of Science, Beirut Arab University, Beirut 11-5020, Lebanon[5]

[c]Department of Physics, Northeastern University, Boston, MA 02115-5000, USA

[d]Department of Physics, Faculty of Science, Alexandria University, Alexandria 21511, Egypt

Abstract

An analysis is given of the chromoelectric dipole moment of quarks and of the neutron in an MSSM extension where the matter sector contains an extra vectorlike generation of quarks and mirror quarks. The analysis includes contributions to the CEDM from the exchange of the W and the Z bosons, from the exchange of charginos and neutralinos and the gluino. Their contribution to the EDM of quarks is investigated. The interference between the MSSM sector and the new sector with vectorlike quarks is investigated. It is shown that inclusion of the vectorlike quarks can modify the quark EDMs in a significant way. Further, this interference also provides a probe of the vectorlike quark sector. These results are of interest as in the future measurements on the neutron EDM could see an improvement up to two orders of magnitude over the current experimental limits and provide an instrument for a further probe of new physics beyond the standard model.

Keywords: Chromoelectric Dipole Moment, quark CEDM, MSSM, vector multiplet
PACS numbers: 12.60.-i, 14.60.Fg

---

*Email: tibrahim@zewailcity.edu.eg
†Email: nath@neu.edu
‡Email: anas.zorik@alexU.edu.eg
[4]Permanent address: Department of Physics, Faculty of Science, University of Alexandria, Alexandria 21511, Egypt
[5]Email: abouibrahim.a@husky.neu.edu

1 Introduction

New sources of CP violation beyond those that exist in the Standard Model are needed to explain baryogenesis and are also worthy of study in their own right as possible probes of beyond the standard model physics (for reviews see e.g., [1, 2, 3, 4]). Such sources can also induce electric dipole moment in elementary particles which can be significantly larger than those expected in the standard model [1, 2]. In this work we are specifically interested in the electric dipole moment (EDM) of the quarks arising from the chromoelectric dipole operator. Thus the electroweak sector of the standard model produces an EDM which is 10^{-30} ecm [5, 6, 7] and it lies beyond the possibility of its observation in the foreseeable future. As mentioned in particle physics models beyond the standard model it is possible to generate much larger values for the EDM. In this work we focus on one such model - an extension of the minimal supersymmetric standard model (MSSM) with a vectorlike multiplet [8]. Such an extension is anomaly free and thus the nice quantum properties of MSSM are maintained. Further, vectorlike multiplets arise in a variety of settings such as in grand unified models and in string and D brane models [8, 10, 11]. Vectorlike generations have been considered by several authors since their discovery would constitute new physics (see, e.g., [9, 10, 11, 12, 13, 14, 15, 16, 17, 18, 19, 20, 21, 22]). Such models have new sources of CP violation and thus can generate substantial size dipole operators. For that reason they are interesting models to consider in the context of lepton and quark EDMs. In a recent work we analyzed the electric dipole operator in such a setting [23] and in this work we analyze the chromoelectric dipole operator in the extended MSSM model and its contribution to the electric dipole moments.

Before discussing the EDM in the new class of models, it is relevant to recall the situation regarding the lepton and quark EDMs in MSSM. Here it is well known that MSSM has a SUSY CP problem, i.e., that the EDM predicted with SUSY phases $O(1)$ are typically in excess of the experimental upper limits. A number of remedies have been offered in the past to remedy this problem. These include a fine tuning of the phases to be small [24], suppression of the EDM by large sparticle masses [25], suppression of the EDM where various contributions conspire to cancel, i.e., the cancellation mechanism [26, 27] as well as other possible remedies (see, e.g., [28]). It has also been suggested that the EDM be used as a probe of new physics beyond the standard model [29, 30, 31, 18, 32]. Specifically the experimental limits on the EDMs can be used as vehicles to probe a new physics regime not accessible otherwise to current and future detectors.

The outline of the rest of the paper is as follows: In section 2 we give a brief description of the model and describe the nature of mixing between the vector generation and the standard three generations of quarks. In section 3.1 we discuss the loop contributions to the chromoelectric dipole moment of the up quark and the down quark that arise from the exchange of the W boson in the loop. In section 3.2 we give an analysis similar to that of section 3.1 for the exchange of the Z boson. In section 3.3 we compute the contribution from the exchange of charginos in the loop and in section 3.4 a similar analysis for the exchange of neutralinos in the loop is given. Finally in section 3.5 we give the analysis for the exchange of the gluino in the loop. In section 4 we discuss the method for the computation of the neutron dipole moment using the quark dipole moments. In section 5 we give a detailed numerical analysis of the contributions to the quark CEDM and to the neutron CEDM for a variety of parameter points in the extended MSSM model. Here we also discuss the use of the neutron EDM as a probe of high mass scales. Conclusions are given in section 6. Further details of the calculational aspects of the analysis are given in sections (7-9).

2 The Model

Here we briefly describe the model and further details are given in the appendix. The model we consider is an extension of MSSM with an additional vectorlike multiplet. Like MSSM the vectorlike extension is free of anomalies and as discussed in section 1 vectorlike multiplets appear in a variety of settings which include grand unified models, string and D brane models. Here we focus on the quark sector where the vectorlike multiplet consists of a fourth generation of quarks and their mirror quarks. Thus the quark sector of the extended MSSM model is given by Eq. (1) and Eq. (2) where,

$$q_{iL} \equiv \begin{pmatrix} t_{iL} \\ b_{iL} \end{pmatrix} \sim \left(3, 2, \frac{1}{6}\right) \;;\quad t^c_{iL} \sim \left(3^*, 1, -\frac{2}{3}\right) \;;\quad b^c_{iL} \sim \left(3^*, 1, \frac{1}{3}\right) \;;\quad i = 1,2,3,4. \tag{1}$$

$$Q^c \equiv \begin{pmatrix} B^c_L \\ T^c_L \end{pmatrix} \sim \left(3^*, 2, -\frac{1}{6}\right) \;;\; T_L \sim \left(3, 1, \frac{2}{3}\right) \;;\; B_L \sim \left(3^*, 1, -\frac{1}{3}\right). \tag{2}$$

The numbers in the braces show the properties under $SU(3)_C \times SU(2)_L \times U(1)_Y$ where the first two entries label the representations for $SU(3)_C$ and $SU(2)_L$ and the last one gives the value of the hypercharge normalized so that $Q = T_3 + Y$. We allow the mixing of the vectorlike generation with the first three generations. Specifically we will focus on the mixings of the mirrors in the vectorlike generation with the first three generations. Details of these mixings are given in Eq. (43). Here we display some relevant features. In the up quark sector we choose a basis as follows

$$\bar{\xi}_R^T = \begin{pmatrix}\bar{t}_R & \bar{T}_R & \bar{c}_R & \bar{u}_R & \bar{t}_{4R}\end{pmatrix}, \quad \xi_L^T = \begin{pmatrix}t_L & T_L & c_L & u_L & \bar{t}_{4L}\end{pmatrix}. \tag{3}$$

and we write the mass term so that

$$-\mathcal{L}_m^u = \bar{\xi}_R^T (M_u) \xi_L + \text{h.c.}, \tag{4}$$

The interaction of Eq. (43) lead to the up-quark mass matrix M_u which is given by

$$M_u = \begin{pmatrix} y'_1 v_2/\sqrt{2} & h_5 & 0 & 0 & 0 \\ -h_3 & y_2 v_1/\sqrt{2} & -h'_3 & -h''_3 & -h_6 \\ 0 & h'_5 & y'_3 v_2/\sqrt{2} & 0 & 0 \\ 0 & h''_5 & 0 & y'_4 v_2/\sqrt{2} & 0 \\ 0 & h_8 & 0 & 0 & y'_5 v_2/\sqrt{2} \end{pmatrix}. \tag{5}$$

This mass matrix is not hermitian and a bi-unitary transformation is needed to diagonalize it. Thus one has

$$D_R^{u\dagger}(M_u) D_L^u = \text{diag}(m_{u_1}, m_{u_2}, m_{u_3}, m_{u_4}, m_{u_5}). \tag{6}$$

Under the bi-unitary transformations the basis vectors transform so that

$$\begin{pmatrix} t_R \\ T_R \\ c_R \\ u_R \\ t_{4R} \end{pmatrix} = D_R^u \begin{pmatrix} u_{1_R} \\ u_{2_R} \\ u_{3_R} \\ u_{4_R} \\ u_{5_R} \end{pmatrix}, \quad \begin{pmatrix} t_L \\ T_L \\ c_L \\ u_L \\ t_{4L} \end{pmatrix} = D_L^u \begin{pmatrix} u_{1_L} \\ u_{2_L} \\ u_{3_L} \\ u_{4_L} \\ u_{5_L} \end{pmatrix}. \tag{7}$$

A similar analysis can be carried out for the down quarks. Here we choose the basis set as

$$\bar{\eta}_R^T = \begin{pmatrix}\bar{b}_R & \bar{B}_R & \bar{s}_R & \bar{d}_R & \bar{b}_{4R}\end{pmatrix}, \quad \eta_L^T = \begin{pmatrix}b_L & B_L & s_L & d_L & b_{4L}\end{pmatrix}. \tag{8}$$

In this basis the down quark mass terms are given by

$$-\mathcal{L}_m^d = \bar{\eta}_R^T (M_d) \eta_L + \text{h.c.}, \tag{9}$$

where using the interactions of Eq. (43), M_d has the following form

$$M_d = \begin{pmatrix} y_1 v_1/\sqrt{2} & h_4 & 0 & 0 & 0 \\ h_3 & y_2' v_2/\sqrt{2} & h_3' & h_3'' & h_6 \\ 0 & h_4' & y_3 v_1/\sqrt{2} & 0 & 0 \\ 0 & h_4'' & 0 & y_4 v_1/\sqrt{2} & 0 \\ 0 & h_7 & 0 & 0 & y_5 v_1/\sqrt{2} \end{pmatrix} . \tag{10}$$

In general $h_3, h_4, h_5, h_3', h_4', h_5', h_3'', h_4'', h_5'', h_6, h_7, h_8$ can be complex and we define their phases so that

$$h_k = |h_k| e^{i\chi_k}, \quad h_k' = |h_k'| e^{i\chi_k'}, \quad h_k'' = |h_k''| e^{i\chi_k''} . \tag{11}$$

The squark sector of the model contains a variety of terms including F -type, D-type and SUSY soft breaking terms. The details of these contributions to squark mass square matrices are discussed in section 7.

3 The analysis of Chromoelectric Dipole Moment Operator

The chromoelectric dipole moment $\tilde{d}^C$ is the coefficient of the effective dimension 5 operator which is defined by

$$\mathcal{L}_I = -\frac{i}{2} \tilde{d}^C_q \bar{q} \sigma_{\mu\nu} \gamma_5 T^a q G^{\mu\nu a}, \tag{12}$$

where $G^{\mu\nu a}$ is the gluon field strength and T^a are the $SU(3)$ generators. The quarks will have five different contributions to the CEDM arising from the W, Z, gluino, chargino and neutralino exchanges. We denote these contributions by $\tilde{d}^C_u(W)$, $\tilde{d}^C_u(Z)$, $\tilde{d}^C_u(\tilde{g})$, $\tilde{d}^C_u(\chi^+)$ and $\tilde{d}^C_u(\chi^0)$. We discuss each of these contributions below.

3.1 W exchange contribution to quark CEDM

For the up quark the W- exchange contribution arises from the left diagram of Fig. (1) using the interaction of Eq. (13), i.e.,

$$-\mathcal{L}_{dWu} = W^\dagger_\rho \sum_{i=1}^{5} \sum_{j=1}^{5} \bar{u}_j \gamma^\rho [G^W_{L_{ji}} P_L + G^W_{R_{ji}} P_R] d_i + \text{h.c.}, \tag{13}$$

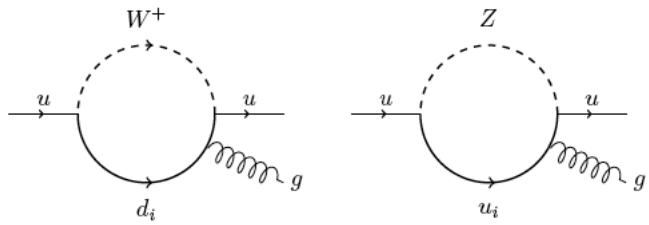

Figure 1: W and Z exchange contributions to the CEDM of the up quark. Similar exchange contributions exist for the CEDM of the down quark where u and d are interchanged and W^+ is replaced by W^- in the diagrams above.

where G_L^W and G_R^W are defined in section 8. The contribution of the W-exchange graph to $\tilde{d}_u^C$ is given by

$$\tilde{d}_u^C(W) = \frac{g_s}{16\pi^2} \sum_{i=1}^{5} \frac{m_{d_i}}{m_W^2} \mathrm{Im}(G_{L4i}^W G_{R4i}^{W*}) I_1\left(\frac{m_{d_i}^2}{m_W^2}, \frac{m_{u_4}^2}{m_W^2}\right), \tag{14}$$

where $I_1(r_1, r_2)$ is a form factor given by

$$I_1(r_1, r_2) = \int_0^1 dx \frac{(4 + r_1 - r_2)x - 4x^2}{1 + (r_1 - r_2 - 1)x + r_2 x^2}. \tag{15}$$

In the limit when r_2 is very small as the case here, this integral gives the closed form

$$I_1(r_1, 0) = \frac{2}{(1 - r_1)^2}\left[1 + \frac{1}{4}r_1 + \frac{1}{4}r_1^2 + \frac{3r_1 \ln r_1}{2(1 - r_1)}\right]. \tag{16}$$

The W contribution to the down quark CEDM is given by

$$\tilde{d}_d^C(W) = \frac{g_s}{16\pi^2} \sum_{i=1}^{5} \frac{m_{u_i}}{m_W^2} \mathrm{Im}(G_{Li4}^{W*} G_{Ri4}^{W}) I_1\left(\frac{m_{u_i}^2}{m_W^2}, \frac{m_{d_4}^2}{m_W^2}\right). \tag{17}$$

3.2 Z exchange contribution to quark CEDM

For the Z boson exchange the interactions that enter with the up type quarks are given by

$$-\mathcal{L}_{uuZ} = Z_\rho \sum_{j=1}^{5} \sum_{i=1}^{5} \bar{u}_j \gamma^\rho [C_{L_{ji}}^{uZ} P_L + C_{R_{ji}}^{uZ} P_R] u_i, \tag{18}$$

where the couplings C_L^{uZ} and C_R^{uZ} are defined in section 8. Using this interaction the computation of the Z exchange contributions to the up quarks is given by the loop diagram to the right in Fig. (1). Its contribution is

$$\tilde{d}_u^C(Z) = \frac{g_s}{16\pi^2}\sum_{i=1}^{5}\frac{m_{u_i}}{m_Z^2}\mathrm{Im}(C_{L_{4i}}^{uZ}C_{R_{4i}}^{uZ*})I_1\left(\frac{m_{u_i}^2}{m_Z^2},\frac{m_{u_4}^2}{m_Z^2}\right). \tag{19}$$

For the Z boson exchange, the interactions that enter with the down type quarks are given by

$$-\mathcal{L}_{ddZ} = Z_\rho\sum_{j=1}^{5}\sum_{i=1}^{5}\bar{d}_j\gamma^\rho[C_{L_{ji}}^{dZ}P_L + C_{R_{ji}}^{dZ}P_R]d_i, \tag{20}$$

where the couplings C_L^{dZ} and C_R^{dZ} are as defined in section 8. A calculation similar to that of the up quark CDEM gives a contribution to the d-quark moment so that

$$\tilde{d}_d^C(Z) = \frac{g_s}{16\pi^2}\sum_{i=1}^{5}\frac{m_{d_i}}{m_Z^2}\mathrm{Im}(C_{L_{4i}}^{dZ}C_{R_{4i}}^{dZ*})I_1\left(\frac{m_{d_i}^2}{m_Z^2},\frac{m_{d_4}^2}{m_Z^2}\right). \tag{21}$$

3.3 Chargino exchange contribution to CEDM

In this section we discuss the interactions in the mass diagonal basis involving squarks, charginos and quarks. Thus we have

$$-\mathcal{L}_{u-\tilde{d}-\chi^-} = \sum_{j=1}^{5}\sum_{i=1}^{2}\sum_{k=1}^{10}\bar{u}_j(C_{jik}^{Lu}P_L + C_{jik}^{Ru}P_R)\tilde{\chi}^{ci}\tilde{d}_k + \text{h.c.}, \tag{22}$$

and

$$-\mathcal{L}_{d-\tilde{u}-\chi^-} = \sum_{j=1}^{5}\sum_{i=1}^{2}\sum_{k=1}^{10}\bar{d}_j(C_{jik}^{Ld}P_L + C_{jik}^{Rd}P_R)\tilde{\chi}^{ci}\tilde{u}_k + \text{h.c.}, \tag{23}$$

where the couplings C^{Lu}, C^{Ru}, C^{Ld} and C^{Rd} and are as defined in section 8. The loop contributions to the up -quark CEDM arise from the right diagram of Fig. (2). Their contribution to CEDM of quarks using Eq. (22) and Eq. (23) are given by

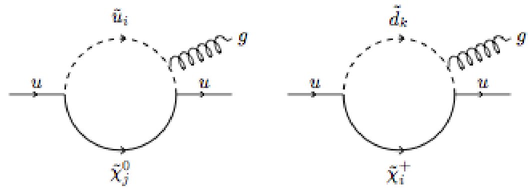

Figure 2: Left diagram: Supersymmetric loop contributions to the CEDM of the up-quark from the diagram involving the exchange of neutralinos and up-squarks. Right diagram: Chargino and down-squark loop contribution to the CEDM of the up quark. Similar loop contributions exist for the CEDM of the down quark, where u and d are interchanged, $\tilde{u}$ and $\tilde{d}$ are interchanged and χ^+ is replaced by χ^- in the diagrams above.

$$\tilde{d}_u^C(\chi^+) = \frac{g_s}{16\pi^2}\sum_{i=1}^{2}\sum_{k=1}^{10}\frac{m_{\chi_i^+}}{M^2_{\tilde{d}_k}}\mathrm{Im}(C^{Lu}_{4ik}C^{Ru*}_{4ik})I_3\left(\frac{m^2_{\chi_i^+}}{M^2_{\tilde{d}_k}}, \frac{m^2_{u_4}}{M^2_{\tilde{d}_k}}\right), \tag{24}$$

$$\tilde{d}_d^C(\chi^+) = \frac{g_s}{16\pi^2}\sum_{i=1}^{2}\sum_{k=1}^{10}\frac{m_{\chi_i^+}}{M^2_{\tilde{u}_k}}\mathrm{Im}(C^{Ld}_{4ik}C^{Rd*}_{4ik})I_3\left(\frac{m^2_{\chi_i^+}}{M^2_{\tilde{u}_k}}, \frac{m^2_{d_4}}{M^2_{\tilde{u}_k}}\right), \tag{25}$$

where $I_3(r_1, r_2)$ is given by

$$I_3(r_1, r_2) = \int_0^1 dx \frac{x - x^2}{1 + (r_1 - r_2 - 1)x + r_2 x^2}. \tag{26}$$

In the limit when r_2 is very small as is the case here we have the closed form

$$I_3(r_1, 0) = \frac{1}{2(r_1 - 1)^2}\left(1 + r_1 + \frac{2r_1 \ln r_1}{1 - r_1}\right). \tag{27}$$

3.4 Neutralino exchange contribution to CEDM

We now discuss the interactions in the mass diagonal basis involving up quarks, up squarks and neutralinos. Thus we have,

$$-\mathcal{L}_{u-\tilde{u}-\chi^0} = \sum_{i=1}^{5}\sum_{j=1}^{4}\sum_{k=1}^{10}\bar{u}_i(C'^L_{uijk}P_L + C'^R_{uijk}P_R)\tilde{\chi}^0_j\tilde{u}_k + \text{h.c.}, \tag{28}$$

The interaction of the down quarks, down squarks and neutralinos is given by

$$-\mathcal{L}_{d-\tilde{d}-\chi^0} = \sum_{i=1}^{4}\sum_{j=1}^{4}\sum_{k=1}^{10} \bar{d}_i (C'^{L}_{dijk} P_L + C'^{R}_{dijk} P_R)\tilde{\chi}^0_j \tilde{d}_k + \text{h.c.}, \tag{29}$$

where the couplings C'^{L} and C'^{R} as given in section 8. Using the interactions of Eq. (28) the neutralino exchange contribution to the CEDM of the up-quark is given by

$$\tilde{d}^C_u(\chi^0) = \frac{g_s}{16\pi^2}\sum_{i=1}^{4}\sum_{k=1}^{10} \frac{m_{\chi^0_i}}{M^2_{\tilde{u}_k}} \text{Im}(C'^{L}_{u4ik} C'^{R*}_{u4ik}) I_3\left(\frac{m^2_{\chi^0_i}}{M^2_{\tilde{u}_k}}, \frac{m^2_{u_4}}{M^2_{\tilde{u}_k}}\right). \tag{30}$$

Similarly using the interactions of Eq. (29) the CEDM of the down quark is given by

$$\tilde{d}^C_d(\chi^0) = \frac{g_s}{16\pi^2}\sum_{i=1}^{4}\sum_{k=1}^{10} \frac{m_{\chi^0_i}}{M^2_{\tilde{d}_k}} \text{Im}(C'^{L}_{d4ik} C'^{R*}_{d4ik}) I_3\left(\frac{m^2_{\chi^0_i}}{M^2_{\tilde{d}_k}}, \frac{m^2_{d_4}}{M^2_{\tilde{d}_k}}\right), \tag{31}$$

3.5 Gluino exchange contribution to CEDM

$$-\mathcal{L}_{q\tilde{q}\tilde{g}} = \sqrt{2} g_s \sum_{j=1}^{3}\sum_{k=1}^{3}\sum_{a=1}^{8}\sum_{l=1}^{5}\sum_{m=1}^{10} T^a_{jk} \bar{q}^j_l [C_{L_{lm}} P_L + C_{R_{lm}} P_R] \tilde{g}_a \tilde{q}^k_m + \text{h.c.}, \tag{32}$$

where the couplings $C_{L_{lm}}$ and $C_{R_{lm}}$ are defined in section 8. Using Eq. (32) the gluino exchange contribution to the up quark CEDM arising from the loop diagrams of Fig. 3 is given by

$$\tilde{d}^C_u(\tilde{g}) = \frac{g_s \alpha_s}{12\pi^2}\sum_{m=1}^{10} \frac{m_{\tilde{g}}}{M^2_{\tilde{u}_m}} \text{Im}(K_{L_{um}} K^*_{R_{um}}) I_5\left(\frac{m^2_{\tilde{g}}}{M^2_{\tilde{u}_m}}, \frac{m^2_{u4}}{M^2_{\tilde{u}_m}}\right). \tag{33}$$

Similarly using Eq. (32) the gluino contribution to the down quark CEDM is given by

$$\tilde{d}^C_d(\tilde{g}) = \frac{g_s \alpha_s}{12\pi^2}\sum_{m=1}^{10} \frac{m_{\tilde{g}}}{M^2_{\tilde{d}_m}} \text{Im}(K_{L_{dm}} K^*_{R_{dm}}) I_5\left(\frac{m^2_{\tilde{g}}}{M^2_{\tilde{d}_m}}, \frac{m^2_{d4}}{M^2_{\tilde{d}_m}}\right). \tag{34}$$

Here $K_{L_{qm}}$ and $K_{R_{qm}}$ are given by

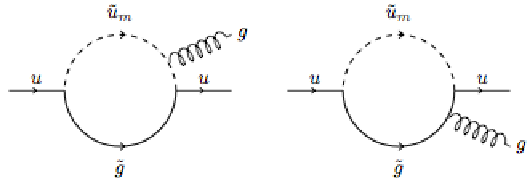

Figure 3: Left diagram: Supersymmetric loop contributions to the CEDM of the up-quark arising from the exchange of gluino and up squarks with the gluon emission from the internal up squark line. Right diagram: Same as left diagram except that the gluon emission is from the internal gluino line. Similar loop contributions exist for the CEDM of the down quark, where u and d are interchanged, $\tilde{u}$ and $\tilde{d}$ are interchanged.

$$K_{L_{qm}} = (D^{q*}_{R24}\tilde{D}^{q}_{4m} - D^{q*}_{R54}\tilde{D}^{q}_{10m} - D^{q*}_{R44}\tilde{D}^{q}_{8m} - D^{q*}_{R34}\tilde{D}^{q}_{6m} - D^{q*}_{R14}\tilde{D}^{q}_{3m})e^{-i\xi_3/2}\,, \tag{35}$$

and

$$K_{R_{qm}} = (D^{q*}_{L44}\tilde{D}^{q}_{7m} + D^{q*}_{L54}\tilde{D}^{q}_{9m} + D^{q*}_{L34}\tilde{D}^{q}_{5m} + D^{q*}_{L14}\tilde{D}^{q}_{1m} - D^{q*}_{L24}\tilde{D}^{q}_{2m})e^{i\xi_3/2}\,, \tag{36}$$

where $I_5(r_1, r_2)$ is the loop function defined by

$$I_5(r_1, r_2) = \int_0^1 dx \frac{x + 8x^2}{1 + (r_1 - r_2 - 1)x + r_2 x^2}\,. \tag{37}$$

In the limit where r_2 is very small as is the case here we get the closed form

$$I_5(r_1, 0) = \frac{1}{2(r_1 - 1)^2}\left(10r_1 - 26 + \frac{2r_1 \ln r_1}{1 - r_1} - \frac{18 \ln r_1}{1 - r_1}\right). \tag{38}$$

4 The neutron CEDM

As discussed in the previous section, the total contribution to CEDM of the quarks consists of five contributions arising from the exchange of the W, the Z, the charginos, the neutralinos, and the gluino, so that

$$\tilde{d}^C_q = \tilde{d}^C_q(W) + \tilde{d}^C_q(Z) + \tilde{d}^C_q(\chi^+) + \tilde{d}^C_q(\chi^0) + \tilde{d}^C_q(\tilde{g}), \quad q = u, d\,. \tag{39}$$

The contribution of the chromoelectric operator to the EDMs of quarks can be computed using dimensional analysis [34]. The contribution to the quark EDM arising from $\tilde{d}_q^C$ is given by

$$d_q^C = \frac{e}{4\pi}\eta^C \tilde{d}_q^C\,, \tag{40}$$

where η^C is approximately equal to 3.4. The factor η^C brings the electric dipole moment from the electroweak scale down to the hadronic scale where it can be compared with experiment. To obtain the contribution to the neutron EDM from the quark EDM, we use the non-relativistic $SU(6)$ quark model which gives

$$d_n^C = \frac{1}{3}[4d_d^C - d_u^C]\,. \tag{41}$$

5 Numerical analysis of neutron EDM

The current experimental limit on the EDM of the neutron is [35]

$$|d_n| < 2.9 \times 10^{-26}\ e\text{cm} \quad (90\%\ \text{CL}). \tag{42}$$

It is expected that a higher sensitivity by as much as two orders of magnitude more sensitive than the current limit may be achievable in the future [36].

We present now a numerical analysis of the neutron CEDM first for the case of MSSM and next for the MSSM extension. The first analysis involves no mixing with the mirror generation and with the fourth sequential generation and the only CP phases that appear are those from the MSSM sector. Thus in this case all the mixing parameters, given in Eq. (11), are set to zero. The second analysis is for the MSSM extension where the mixings of the mirror generation and of the fourth sequential generation with the three generations are switched on. The results are given in Table 2 and Figs. 4-11. In the analysis, in the squark sector we assume $m_0^{u^2} = M_{\tilde{T}}^2 = M_{\tilde{t}_1}^2 = M_{\tilde{t}_2}^2 = M_{\tilde{t}_3}^2$ and $m_0^{d^2} = M_{\tilde{1}L}^2 = M_{\tilde{B}}^2 = M_{\tilde{b}_1}^2 = M_{\tilde{Q}}^2 = M_{\tilde{2}L}^2 = M_{\tilde{b}_2}^2 = M_{\tilde{3}L}^2 = M_{\tilde{b}_3}^2$. To simplify the numerical analysis further we assume $m_0^u = m_0^d = m_0$. Additionally the trilinear couplings are chosen so that: $A_0^u = A_t = A_T = A_c = A_u = A_{4t}$ and $A_0^d = A_b = A_B = A_s = A_d = A_{4b}$. The input parameters are such that the sparticle spectrum that enters the loop are consistent with the current experimental limits from the LHC in each of the cases, i.e., with or without mixing.

Contribution	(i)		(ii)	
	Up	Down	Up	Down
Chargino, $d_q^{\chi^\pm}$	2.49×10^{-29}	-1.29×10^{-26}	2.16×10^{-29}	-2.08×10^{-26}
Neutralino, $d_q^{\chi^0}$	-2.49×10^{-32}	4.75×10^{-29}	-2.90×10^{-32}	5.47×10^{-29}
Gluino, d_q^g	3.42×10^{-29}	-4.24×10^{-28}	7.49×10^{-28}	2.06×10^{-26}
Total, d_q	5.90×10^{-29}	-1.32×10^{-26}	7.71×10^{-28}	-1.42×10^{-28}
EDM, d_n^E	-2.70×10^{-26}		-6.83×10^{-28}	
Chargino, $d_q^C(\chi^\pm)$	-3.41×10^{-30}	-2.15×10^{-27}	-2.89×10^{-30}	-3.40×10^{-27}
Neutralino, $d_q^C(\chi^0)$	-4.54×10^{-32}	-1.73×10^{-28}	-5.30×10^{-32}	-2.00×10^{-28}
Gluino, $d_q^C(\tilde{g})$	5.51×10^{-29}	1.37×10^{-27}	1.21×10^{-27}	-6.63×10^{-26}
Total, d_q^C	1.40×10^{-29}	-2.58×10^{-28}	3.26×10^{-28}	-1.89×10^{-26}
CEDM, d_n^C	-3.49×10^{-28}		-2.53×10^{-26}	

Table 1: An exhibition of the chargino, neutralino and gluino exchange contributions to the quark and the neutron EDM, CEDM and their sum for the case when there is no mixing of the vectorlike generation with the three generations. The analysis is for two benchmark points (i) and (ii). Benchmark (i): $\theta_\mu = 3.3 \times 10^{-3}$, $\xi_3 = 1 \times 10^{-3}$. Benchmark (ii): $\theta_\mu = 4.7 \times 10^{-3}$, $\xi_3 = 3.6$. The common parameters are: $\tan\beta = 40$, $m_0 = m_0^u = m_0^d = 3000$, $|m_1| = 185$, $|m_2| = 220$, $|A_0^u| = 680$, $|A_0^d| = 600$, $|\mu| = 400$, $m_g = 1000$, $|h_3| = |h_3'| = |h_3''| = |h_4| = |h_4'| = |h_4''| = |h_5| = |h_5'| = |h_5''| = |h_6| = |h_7| = |h_8| = 0$, $\xi_1 = 2 \times 10^{-2}$, $\xi_2 = 2 \times 10^{-3}$, $\alpha_{A_0^u} = 2 \times 10^{-2}$, $\alpha_{A_0^d} = 3$. All masses are in GeV, all phases in rad and the electric dipole moment in $e$cm.

We discuss now in further detail the cases without and with mixing with the vectorlike generation. We begin with the case with no mixing. In table 1, we give the individual contributions to the up and down quark EDM and CEDM, namely, the chargino, the neutralino and the gluino contributions. The W and Z contributions are not shown since they are absent in this case of no mixing with the vectorlike generation and the fourth sequential generation. The different contributions are given for two benchmark points (i) and (ii), where in the first, the neutron EDM dominates the neutron CEDM and in the second, the opposite is the case. The chargino and gluino contributions are the main contributors, while the neutralino contribution is suppressed. Note that the total neutron EDM, $|d_n|$, obtained by adding d_n^E and d_n^C in the table satisfy Eq. (42). Another observation is the largeness of the down quark contribution in comparison with its up quark counterpart. This is attributed to the large value of $\tan\beta$ which tends to enhance the down quark couplings.

Contribution	(i) Up	(i) Down	(ii) Up	(ii) Down
Chargino, $d_q^{\chi^\pm}$	7.65×10^{-30}	-6.91×10^{-27}	7.08×10^{-30}	-8.27×10^{-27}
Neutralino, $d_q^{\chi^0}$	3.93×10^{-32}	6.90×10^{-30}	3.91×10^{-32}	7.32×10^{-30}
Gluino, d_q^g	-2.01×10^{-28}	-5.35×10^{-27}	2.25×10^{-28}	5.91×10^{-27}
W Boson, d_q^W	3.77×10^{-30}	3.46×10^{-28}	3.77×10^{-30}	3.46×10^{-28}
Z Boson, d_q^Z	8.02×10^{-31}	3.05×10^{-29}	8.02×10^{-31}	3.05×10^{-29}
Total, d_q	-1.88×10^{-28}	-1.19×10^{-26}	2.37×10^{-28}	-1.97×10^{-27}
EDM, d_n^E	-2.41×10^{-26}		-4.13×10^{-27}	
Chargino, $d_q^C(\chi^\pm)$	-7.66×10^{-31}	-8.98×10^{-28}	-6.95×10^{-31}	-1.07×10^{-27}
Neutralino, $d_q^C(\chi^0)$	7.17×10^{-32}	-2.52×10^{-29}	7.14×10^{-32}	-2.68×10^{-29}
Gluino, $d_q^C(\tilde{g})$	-4.57×10^{-28}	2.44×10^{-26}	5.13×10^{-28}	-2.70×10^{-26}
W Boson, $d_q^C(W)$	-2.97×10^{-30}	2.29×10^{-28}	-2.97×10^{-30}	2.29×10^{-28}
Z Boson, $d_q^C(Z)$	1.46×10^{-30}	-1.11×10^{-28}	1.46×10^{-30}	-1.11×10^{-28}
Total, d_q^C	-1.24×10^{-28}	6.38×10^{-27}	1.38×10^{-28}	-7.56×10^{-27}
CEDM, d_n^C	8.54×10^{-27}		-1.01×10^{-26}	

Table 2: An exhibition of the chargino, neutralino, gluino, W and Z exchange contributions to the quark and the neutron EDM, CEDM and their sum for the case when there is mixing of the vectorlike generation with the three generations. The analysis is for two benchmark points (i) and (ii). Benchmark (i): $\theta_\mu = 4\times10^{-3}$, $\xi_3 = 1.12$. Benchmark (ii): $\theta_\mu = 4.6\times10^{-3}$, $\xi_3 = 4.71$. The common parameters are: $\tan\beta = 40$, $m_0 = m_0^u = m_0^d = 5500$, $|m_1| = 185$, $|m_2| = 220$, $|A_0^u| = 680$, $|A_0^d| = 600$, $|\mu| = 400$, $m_g = 1100$, $m_T = 300$, $m_B = 240$, $m_{4t} = 320$, $m_{4b} = 280$, $|h_3| = 1.58$, $|h'_3| = 6.34 \times 10^{-2}$, $|h''_3| = 1.97 \times 10^{-2}$, $|h_4| = 4.42$, $|h'_4| = 5.07$, $|h''_4| = 12.87$, $|h_5| = 6.6$, $|h'_5| = 2.67$, $|h''_5| = 1.86\times10^{-1}$, $|h_6| = 1000$, $|h_7| = 1000$, $|h_8| = 1000$, $\xi_1 = 2 \times 10^{-2}$, $\xi_2 = 2 \times 10^{-3}$, $\alpha_{A_0^u} = 2 \times 10^{-2}$, $\alpha_{A_0^d} = 3$, $\chi_3 = 2 \times 10^{-2}$, $\chi'_3 = 1 \times 10^{-3}$, $\chi''_3 = 4\times10^{-3}$, $\chi_4 = 7\times10^{-3}$, $\chi'_4 = \chi''_4 = 1\times10^{-3}$, $\chi_5 = 9\times10^{-3}$, $\chi'_5 = 5\times10^{-3}$, $\chi''_5 = 2\times10^{-3}$, $\chi_6 = \chi_7 = \chi_8 = 5 \times 10^{-3}$. All masses are in GeV, all phases in rad and the electric dipole moment in $e$cm.

Next we consider the case with mixings. The results are presented in table 2 for two benchmark points (i) and (ii). Here in addition to the chargino, the neutralino and the gluino exchanges one also has W and Z exchanges. The analysis shows the dominance of the EDM over the CEDM for benchmark (i) while opposite is the case for benchmark (ii). The total EDM for each benchmark point satisfies the experimental constraints of Eq. (42). Here we note that the EDM and CEDM are constrained not only by the experimental limits on the MSSM spectrum, but also by the limits on new quarks. Thus for the benchmarks presented in Table 2, the vectorlike quarks have masses gotten by diagonalization of the matrices of Eq. (5) and Eq. (10) and are given in Table 3. The results of Eq. 3 are consistent with [37]. More stringent constraints on these masses will be available at the LHC RUN-II.

Mirror Up Quark	$m_{t'} = 1037$ GeV
Mirror Down Quark	$m_{b'} = 740$ GeV
Fourth G Up Quark	$m_4^{\text{up}} = 1057$ GeV
Fourth G Down Quark	$m_4^{\text{down}} = 1260$ GeV

Table 3: An exhibition of the masses of the heavy extra quarks corresponding to the parameter space of table 2.

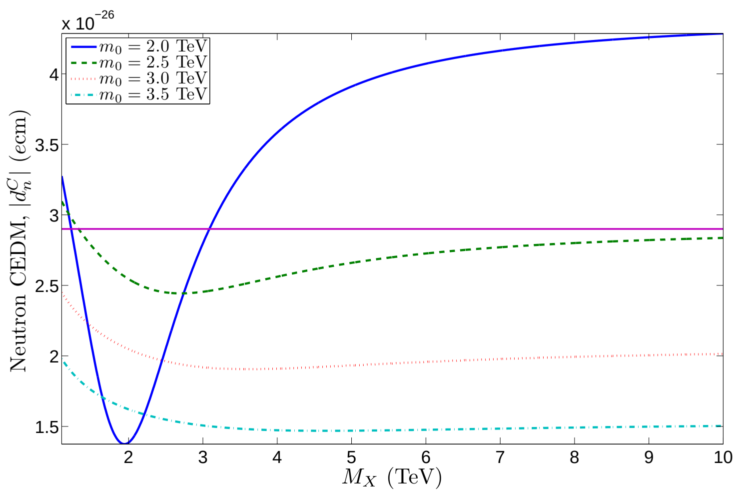

Figure 4: Variation of neutron CEDM $|d_n^C|$ versus M_X ($M_X = |h_6| = |h_7| = |h_8|$), for four values of m_0. From top to bottom at $M_X = 4$ TeV, $m_0 = m_0^u = m_0^d = 2.0, 2.5, 3.0, 3.5$ TeV. Other parameters have the values $\tan\beta = 14$, $|m_1| = 185$, $|m_2| = 220$, $|\mu| = 350$, $|A_0^u| = 680$, $|A_0^d| = 600$, $m_T = 300$, $m_B = 260$, $m_g = 1000$, $m_{4t} = 320$, $m_{4b} = 280$, $|h_3| = 1.58$, $|h_3'| = |h_3''| = RM_X$, $|h_4| = 4.42$, $|h_4'| = |h_4''| = RM_X$, $|h_5| = 6.6$, $|h_5'| = |h_5''| = RM_X$, $R = 1 \times 10^{-3}$, $\theta_\mu = 3.98$, $\xi_1 = \xi_2 = 4.52$, $\xi_3 = 2.42$, $\alpha_{A_0^u} = 5.0$, $\alpha_{A_0^d} = 1.14$, $\chi_3 = 2.38$, $\chi_3' = 4.92$, $\chi_3'' = 2.58$, $\chi_4 = 4.86$, $\chi_4' = 1.6$, $\chi_4'' = 1.37$, $\chi_5 = 1.14$, $\chi_5' = 4.39$, $\chi_5'' = 2.38$, $\chi_6 = 4.92$, $\chi_7 = 2.58$, $\chi_8 = 4.86$. All masses are in GeV and phases in rad.

Next we give an analysis of the quark CEDMs dependence on the mass scales as well as on the CP phases both in the MSSM sector as well as the new sector. Thus the CEDM depends on the mass scale of the vectorlike sector and in the MSSM sector it depends on the universal scalar mass m_0, and on the gaugino mass scales. Further, it has dependence on several CP phases both from the MSSM sector as well as from the vectorlike sector. We discuss the dependence of the CEDM on the mass scales first, and specifically on the mass scales M_X (from the vectorlike sector) and on m_0 and on m_g.

Fig. 4 gives the dependence of the effect of the vectorlike generation on CEDM where we exhibit CEDM vs M_X, where $M_X = |h_6| = |h_7| = |h_8|$ and that $|h'_3| = |h''_3| = |h'_4| = |h''_4| = |h'_5| = |h''_5| = RM_X$ while $R = 1 \times 10^{-3}$. We note that the allowed range of values for R is highly constrained. Thus smaller values of R will not produce interesting results while larger values are likely to upset the quark masses for the first three generations. The analysis shows that CEDM lower than the upper limit can be obtained and masses in the TeV range may be probed using the constraint given by Eq. (42) which should undergo further refinements in the future. The curve corresponding to $m_0 = 2$ TeV is characterized by a dip at $M_X \sim 1.9$ TeV. This dip quickly widens and is replaced by a shallow drop for $m_0 = 2.5$ TeV and then disappears completely for larger values of m_0. The variation of the CEDM eventually levels off for higher values of M_X and m_0. Further analysis shows that the dip is caused by a sudden drop in the mass of the lightest up squark mass for $M_X \sim 1.9$ TeV in this region of the parameter space. The analysis of the dip is rather involved but arises as a result of the competition among the different components of the chromoelectric dipole moment operators, i.e, the W, Z, chargino, neutralino and gluino contributions. The analysis of Fig. 4 makes clear the very sensitive dependence of the CEDM on the vectorlike mass scale and exploration of this dependence is one of the primary motivations of this work.

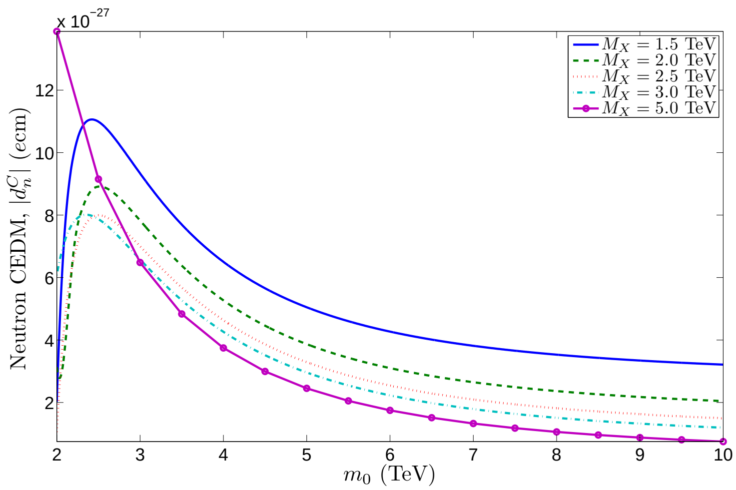

Figure 5: Variation of neutron CEDM $|d_n^C|$ versus the scalar mass m_0 ($m_0 = m_0^u = m_0^d$), for five values of M_X, ($M_X = |h_6| = |h_7| = |h_8|$). From top to bottom at $m_0 = 5$ TeV, $M_X = 1.5, 2.0, 2.5, 3.0, 5$ TeV. Other parameters have the values $\tan\beta = 14$, $|m_1| = 185$, $|m_2| = 220$, $|\mu| = 350$, $|A_0^u| = 680$, $|A_0^d| = 600$, $m_T = 300$, $m_B = 260$, $m_g = 1000$, $m_{4t} = 320$, $m_{4b} = 280$, $|h_3| = 1.58$, $|h_3'| = |h_3''| = RM_X$, $|h_4| = 4.42$, $|h_4'| = |h_4''| = RM_X$, $|h_5| = 6.6$, $|h_5'| = |h_5''| = RM_X$, $R = 1\times10^{-3}$, $\theta_\mu = 3.8$, $\xi_1 = \xi_2 = 4.52$, $\xi_3 = 2.42$, $\alpha_{A_0^u} = 5.0$, $\alpha_{A_0^d} = 1.14$, $\chi_3 = 2.38$, $\chi_3' = 4.92$, $\chi_3'' = 2.58$, $\chi_4 = 4.86$, $\chi_4' = 1.6$, $\chi_4'' = 1.37$, $\chi_5 = 1.14$, $\chi_5' = 4.39$, $\chi_5'' = 2.38$, $\chi_6 = 4.92$, $\chi_7 = 2.58$, $\chi_8 = 4.86$. All masses are in GeV and phases in rad.

Another way for looking at Fig. 4 is to plot the CEDM against m_0 for several values of M_X while R is fixed at 1×10^{-3} in the same region of parameter space. This is done in Fig. 5. The plot shows peaks between 2 and 3 TeV and then the CEDM decreases gradually for increasing values of m_0. The peak is more pronounced for small values of M_X and disappears for larger values (for $M_X = 5$ TeV, here). The peaks occur in regions where m_0 and M_X are comparable in size as shown in this region. All values of the CEDM obtained in this region of the parameter space lie below the current upper limit.

In Fig. 4 we investigated the dependence of CEDM on the vectorlike mass M_X and found that there is a very significant dependence of the CEDM on M_X. It is of interest also to examine if the EDM shows a similar dependence on M_X. In Fig. 4 we exhibit this dependence where $|d_n^E|$ is plotted against M_X for the same set of m_0 values as in Fig. 4. Again as in the case of CEDM we find that EDM also has a sensitive dependence on M_X. We note here that the analysis of this work for EDM is more general than the analysis of [23]. Thus in [23]

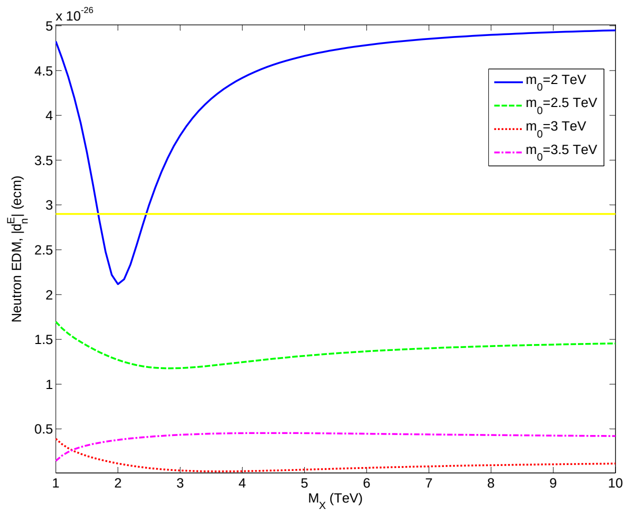

Figure 6: Variation of neutron EDM $|d_n^E|$ versus M_X ($M_X = |h_6| = |h_7| = |h_8|$), for four values of m_0. From top to bottom at $M_X = 1$ TeV, $m_0 = m_0^u = m_0^d = 2.0$, 2.5, 3.0, 3.5 TeV. Other parameters have the values $\tan\beta = 15$, $|m_1| = 185$, $|m_2| = 220$, $|\mu| = 350$, $|A_0^u| = 680$, $|A_0^d| = 600$, $m_T = 300$, $m_B = 260$, $m_g = 1000$, $m_{4t} = 320$, $m_{4b} = 280$, $|h_3| = 1.58$, $|h_3'| = |h_3''| = RM_X$, $|h_4| = 4.42$, $|h_4'| = |h_4''| = RM_X$, $|h_5| = 6.6$, $|h_5'| = |h_5''| = RM_X$, $R = 1 \times 10^{-3}$, $\theta_\mu = 5 \times 10^{-3}$, $\xi_1 = 2 \times 10^{-2}$, $\xi_2 = 2 \times 10^{-3}$, $\xi_3 = 4.0$, $\alpha_{A_0^u} = 2 \times 10^{-2}$, $\alpha_{A_0^d} = 3.0$, $\chi_3 = 2 \times 10^{-2}$, $\chi_3' = 1 \times 10^{-3}$, $\chi_3'' = 4 \times 10^{-3}$, $\chi_4 = 7 \times 10^{-3}$, $\chi_4' = \chi_4'' = 1 \times 10^{-3}$, $\chi_5 = 9 \times 10^{-3}$, $\chi_5' = 5 \times 10^{-3}$, $\chi_5'' = 2 \times 10^{-3}$, $\chi_6 = \chi_7 = \chi_8 = 5 \times 10^{-3}$. All masses are in GeV and phases in rad.

we considered only the mixings of the three generations with the mirror generation so that the quark matrices were 4×4 and the squark square matrices were 8×8 and the parameter M_X did not appear in that work. On the other hand, in this work we are considering mixing of the three generations with the full vectorlike generation consisting of the mirror and the sequential fourth generation. As a consequence the quark mass matrices are 5×5 and the squark mass squared matrices are 10×10 and this time we have also the dependence on the vectorlike mass M_X. Thus the analysis of this work is more general than of the work of [23].

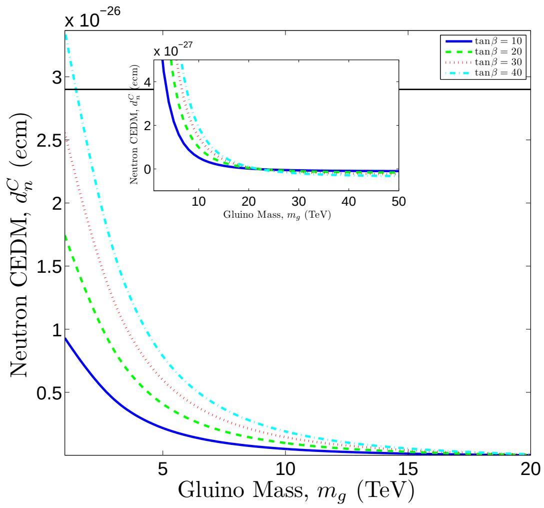

Figure 7: Variation of neutron CEDM d_n^C versus the gluino mass, m_g, for four values of $\tan\beta$. From bottom to top at $m_g = 5$ TeV, $\tan\beta = 10, 20, 30, 40$. Other parameters have the values $|m_1| = 170$, $|m_2| = 220$, $|\mu| = 450$, $|A_0^u| = 680$, $|A_0^d| = 600$, $m_0^u = m_0^d = 3700$, $m_T = 300$, $m_B = 260$, $m_{4t} = 320$, $m_{4b} = 280$, $|h_3| = 1.58$, $|h_3'| = 6.34 \times 10^{-2}$, $|h_3''| = 1.97 \times 10^{-2}$, $|h_4| = 4.42$, $|h_4'| = 5.07$, $|h_4''| = 2.87$, $|h_5| = 6.6$, $|h_5'| = 2.67$, $|h_5''| = 1.86 \times 10^{-1}$, $|h_6| = |h_7| = |h_8| = 1000$, $\theta_\mu = 2.6 \times 10^{-3}$, $\xi_1 = 2 \times 10^{-2}$, $\xi_2 = 2 \times 10^{-3}$, $\xi_3 = 1.6$, $\alpha_{A_0^u} = 2 \times 10^{-2}$, $\alpha_{A_0^d} = 3.0$, $\chi_3 = 2 \times 10^{-2}$, $\chi_3' = 1 \times 10^{-3}$, $\chi_3'' = 4 \times 10^{-3}$, $\chi_4 = 7 \times 10^{-3}$, $\chi_4' = \chi_4'' = 1 \times 10^{-3}$, $\chi_5 = 9 \times 10^{-3}$, $\chi_5' = 5 \times 10^{-3}$, $\chi_5'' = 2 \times 10^{-3}$, $\chi_6 = \chi_7 = \chi_8 = 5 \times 10^{-3}$. All masses are in GeV and phases in rad.

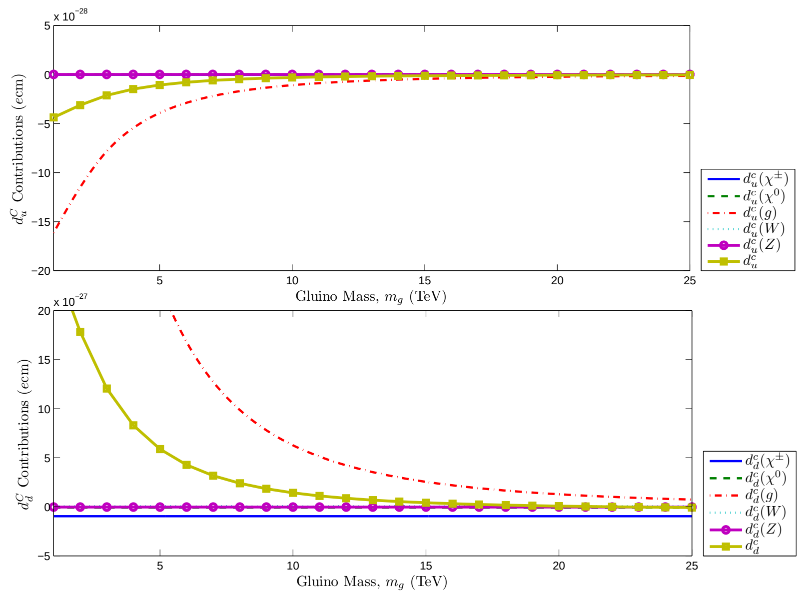

Figure 8: Variation of up and down quark contributions to the neutron CEDM for $\tan\beta = 40$. Other parameters are the same as in Fig. 7.

Next we study the dependence of the CEDM on the gluino mass. This is given in Figs. 7 and 8. Thus in Fig. 7, the variation of the neutron CEDM, d_n^C, is plotted against the gluino mass, m_g. It is shown that CEDM values lower than the current experimental upper limit can be obtained in the given parameter space. The neutron CEDM decreases for increasing values of m_g, but eventually levels off at around zero for some values of $\tan\beta$. However, for other values of $\tan\beta$, (e.g. $\tan\beta = 40$), the neutron CEDM levels off but turns negative. This phenomenon can be understood by analyzing different contributions to the CEDM as shown in Fig. 8. Specifically one finds that the negative contribution to the CEDM arises from the chargino exchange loop contribution, $d_d^c(\chi^{\pm})$. Since we are not applying any GUT constraints, the masses of the chargino and the gluino can be treated as independent parameters and thus as we increase the gluino mass, the chargino contribution remains unchanged and eventually dominates as the gluino mass gets large and makes the CEDM negative for $m_g > 20$ TeV. We note here in passing that the W and Z contributions in this region of the parameter space are negligible compared to the other exchange contributions.

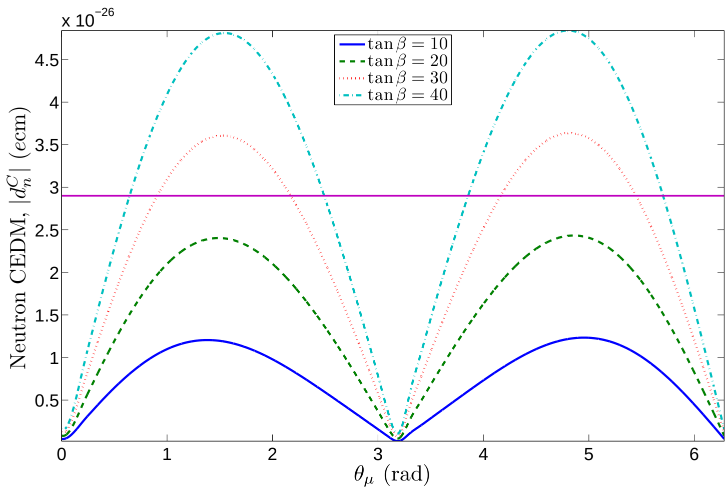

Figure 9: Variation of neutron CEDM $|d_n^C|$ versus θ_μ for four values of $\tan\beta$. From bottom to top at $\theta_\mu = 1$ rad, $\tan\beta = 10, 20, 30, 40$. Other parameters have the values $|m_1| = 170$, $|m_2| = 220$, $|\mu| = 400$, $|A_0^u| = 680$, $|A_0^d| = 600$, $m_0^u = m_0^d = 8000$, $m_g = 1000$, $m_T = 300$, $m_B = 260$, $m_{4t} = 320$, $m_{4b} = 280$, $|h_3| = 1.58$, $|h_3'| = 6.34 \times 10^{-2}$, $|h_3''| = 1.97 \times 10^{-2}$, $|h_4| = 4.42$, $|h_4'| = 5.07$, $|h_4''| = 2.87$, $|h_5| = 6.6$, $|h_5'| = 2.67$, $|h_5''| = 1.86 \times 10^{-1}$, $|h_6| = |h_7| = |h_8| = 1000$, $\xi_1 = 2\times 10^{-2}$, $\xi_2 = 2\times 10^{-3}$, $\xi_3 = 2.6$, $\alpha_{A_0^u} = 2\times 10^{-2}$, $\alpha_{A_0^d} = 3.0$, $\chi_3 = 2\times 10^{-2}$, $\chi_3' = 1\times 10^{-3}$, $\chi_3'' = 4\times 10^{-3}$, $\chi_4 = 7\times 10^{-3}$, $\chi_4' = \chi_4'' = 1\times 10^{-3}$, $\chi_5 = 9\times 10^{-3}$, $\chi_5' = 5\times 10^{-3}$, $\chi_5'' = 2 \times 10^{-3}$, $\chi_6 = \chi_7 = \chi_8 = 5 \times 10^{-3}$. All masses are in GeV and phases in rad.

As discussed already, it is of interest to study the dependence of CEDM on the CP phases in the MSSM sector as well as in the new sector. Fig. 9 shows the variation of the neutron CEDM versus θ_μ, the phase of μ. The CP phases are the source of the CEDM and the sensitivity that the CEDM shows in response to the variation of θ_μ is obvious. The parameter μ appears in the chargino and the neutralino mass matrices. It exists also in the squark mass squared matrices, so one can see that the chargino, the neutralino and the gluino contributions are affected by this parameter and its phase. The electroweak contributions, i.e, W and Z components are independent of the magnitude and the phase of μ. Values of $|d_n^C|$ below the current upper limit can be obtained for several values of $\tan\beta$, whereas values above the limit appear for larger $\tan\beta$.

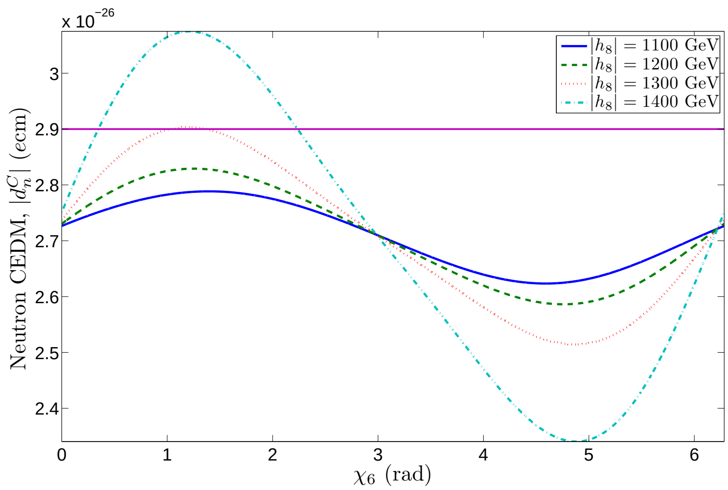

Figure 10: Variation of neutron CEDM $|d_n^C|$ versus χ_6, for four values of $|h_8|$. From bottom to top at $\chi_6 = 1$ rad, $|h_8| = 1100, 1200, 1300, 1400$ GeV. Other parameters have the values $\tan\beta = 34$, $|m_1| = 185$, $|m_2| = 220$, $|\mu| = 350$, $|A_0^u| = 680$, $|A_0^d| = 600$, $m_0^u = m_0^d = 3600$, $m_T = 300$, $m_B = 260$, $m_g = 4000$, $m_{4t} = 320$, $m_{4b} = 280$, $|h_3| = 1.58$, $|h_3'| = 6.34 \times 10^{-2}$, $|h_3''| = 1.97 \times 10^{-2}$, $|h_4| = 4.42$, $|h_4'| = 5.07$, $|h_4''| = 2.87$, $|h_5| = 6.6$, $|h_5'| = 2.67$, $|h_5''| = 1.86 \times 10^{-1}$, $|h_6| = |h_7| = 1100$, $\theta_\mu = 0.1$, $\xi_1 = 2 \times 10^{-2}$, $\xi_2 = 2 \times 10^{-3}$, $\xi_3 = 3.6$, $\alpha_{A_0^u} = 2 \times 10^{-2}$, $\alpha_{A_0^d} = 3.0$, $\chi_3 = 2 \times 10^{-2}$, $\chi_3' = 1 \times 10^{-3}$, $\chi_3'' = 4 \times 10^{-3}$, $\chi_4 = 7 \times 10^{-3}$, $\chi_4' = \chi_4'' = 1 \times 10^{-3}$, $\chi_5 = 9 \times 10^{-3}$, $\chi_5' = 5 \times 10^{-3}$, $\chi_5'' = 2 \times 10^{-3}$, $\chi_7 = \chi_8 = 5 \times 10^{-3}$. All masses are in GeV and phases in rad.

Next we investigate the dependence of CEDM on χ_6 which explores a new sector of the theory as it is the CP phase that arises in interactions involving the mirror quarks and the fourth generation quarks. An analysis of the dependence of CEDM on χ_6 is exhibited in Fig. 10. Aside from h_6, other mass parameters that arise because of the new sector are h_7 and h_8. The dependence of the CEDM on $|h_8|$ is also exhibited in Fig. 10. Quite remarkably CEDM is sensitive to both the mass scale and the phase that enters in the new sector.

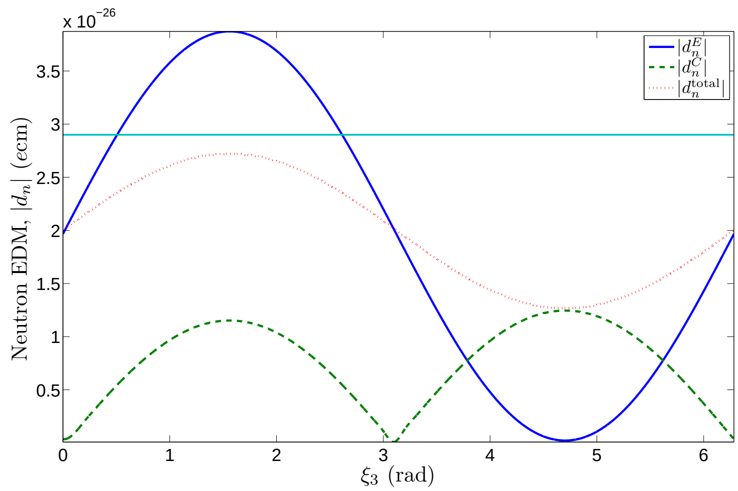

Figure 11: Variation of the neutron EDM, $|d_n^E|$ (solid curve), the neutron CEDM, $|d_n^C|$ (dashed curve), and the total neutron EDM, $|d_n^{\rm total}|$ (dotted curve), versus ξ_3, the phase of the gluino mass, for $\tan\beta = 40$. Other parameters have the values $|m_1| = 185$, $|m_2| = 220$, $|\mu| = 400$, $|A_0^u| = 680$, $|A_0^d| = 600$, $m_0^u = m_0^d = 5000$, $m_T = 300$, $m_B = 260$, $m_g = 1500$, $m_{4t} = 320$, $m_{4b} = 280$, $|h_3| = 1.58$, $|h_3'| = 6.34 \times 10^{-2}$, $|h_3''| = 1.97 \times 10^{-2}$, $|h_4| = 4.42$, $|h_4'| = 5.07$, $|h_4''| = 2.87$, $|h_5| = 6.6$, $|h_5'| = 2.67$, $|h_5''| = 1.86 \times 10^{-1}$, $|h_6| = |h_7| = |h_8| = 1000$, $\theta_\mu = 4.7 \times 10^{-3}$, $\xi_1 = 2 \times 10^{-2}$, $\xi_2 = 2 \times 10^{-3}$, $\alpha_{A_0^u} = 2 \times 10^{-2}$, $\alpha_{A_0^d} = 3.0$, $\chi_3 = 2 \times 10^{-2}$, $\chi_3' = 1\times 10^{-3}$, $\chi_3'' = 4\times 10^{-3}$, $\chi_4 = 7\times 10^{-3}$, $\chi_4' = \chi_4'' = 1\times 10^{-3}$, $\chi_5 = 9\times 10^{-3}$, $\chi_5' = 5\times 10^{-3}$, $\chi_5'' = 2 \times 10^{-3}$, $\chi_6 = \chi_7 = \chi_8 = 5 \times 10^{-3}$. All masses are in GeV and phases in rad.

Finally, it is of interest to look at the total electric dipole moment obtained by adding the electric and the chromoelectric dipole moments. Fig. 11 shows the variation of the EDM, the CEDM and the total EDM against the gluino phase, ξ_3. The analysis of Fig. 11 shows that while the EDM may dominate the CEDM for some values of ξ_3 the opposite may happen for a different range of ξ_3. The analysis also suggests constructive interference between EDM and CEDM in some parts of the parameter space while there is destructive interferences in other parts (i.e., for $0 < \xi_3 < \pi$) leading to the cancellations mechanism [26, 27].

6 Conclusion

In this work we have given an analysis of the chromoelectric dipole moment of quarks and of the neutron arising in an extension of MSSM where there is an additional vectorlike generation of quarks in the matter sector. Such an extension brings in new sources of CP

violation which can contribute to the chromoelectric dipole moment of quarks. The work presented here consists of analytical results on five different types of contributions to the chromoelectric dipole moments of quarks which include both non-supersymmetric as well as supersymmetric loop contributions. In the non-supersymmetric sector we have contributions arising from the exchanges of the W and Z bosons in the loops, while in the supersymmetric sector we have exchanges involving charginos, neutralinos and the gluino in the loop. We have also carried out a detailed numerical analysis of their relative contributions. Specifically it is found that there exists strong interference effects between the MSSM sector and the vectorlike quark sector which can drastically change both the sign and the magnitude of quark EDMs. We have also investigated the possibility that the neutron EDM can be used as probe of the TeV scale physics. These results are of import as future experiment can improve the current limits up to two orders of magnitude and thus the quark EDMs provide an important window to new physics beyond the standard model.
Acknowledgments: PN's research is supported in part by the NSF grant PHY-1314774.

7 Appendix A: Squark mass matrices

In this Appendix we give further details of the model discussed in section 2. As discussed in section 2 we allow for mixing between the vector generation and specifically the mirrors and the standard three generations of quarks. We also allow for mixing between the mirror generation and the fourth sequential generation assuming R parity conservation (for a recent review of R parity see [33]). The superpotential allowing such mixings is given by

$$\begin{aligned}
W = \epsilon_{ij}[&y_1\hat{H}_1^i\hat{q}_{1L}^{j}\hat{b}_{1L}^c + y_1'\hat{H}_2^j\hat{q}_{1L}^{i}\hat{t}_{1L}^c + y_2\hat{H}_1^i\hat{Q}^{cj}\hat{T}_L + y_2'\hat{H}_2^j\hat{Q}^{ci}\hat{B}_L \\
&+ y_3\hat{H}_1^i\hat{q}_{2L}^{j}\hat{b}_{2L}^c + y_3'\hat{H}_2^j\hat{q}_{2L}^{i}\hat{t}_{2L}^c + y_4\hat{H}_1^i\hat{q}_{3L}^{j}\hat{b}_{3L}^c + y_4'\hat{H}_2^j\hat{q}_{3L}^{i}\hat{t}_{3L}^c + y_5\hat{H}_1^i\hat{q}_{4L}^{j}\hat{b}_{4L}^c + y_5'\hat{H}_2^j\hat{q}_{4L}^{i}\hat{t}_{4L}^c] \\
&+ h_3\epsilon_{ij}\hat{Q}^{ci}\hat{q}_{1L}^j + h_3'\epsilon_{ij}\hat{Q}^{ci}\hat{q}_{2L}^j + h_3''\epsilon_{ij}\hat{Q}^{ci}\hat{q}_{3L}^j + h_4\hat{b}_{1L}^c\hat{B}_L + h_5\hat{t}_{1L}^c\hat{T}_L + h_4'\hat{b}_{2L}^c\hat{B}_L \\
&+ h_5'\hat{t}_{2L}^c\hat{T}_L + h_4''\hat{b}_{3L}^c\hat{B}_L + h_5''\hat{t}_{3L}^c\hat{T}_L + h_6\epsilon_{ij}Q^iq_{4L}^j + h_7\hat{b}_{4L}^c\hat{B}_L + h_8\hat{t}_{4L}^c\hat{T}_L - \mu\epsilon_{ij}\hat{H}_1^i\hat{H}_2^j\ , \quad (43)
\end{aligned}$$

Here the couplings are in general complex. Thus, for example, μ is the complex Higgs mixing parameter so that $\mu = |\mu|e^{i\theta_\mu}$. The mass terms for the ups, mirror ups, downs and mirror downs arise from the term

$$\mathcal{L} = -\frac{1}{2}\frac{\partial^2 W}{\partial A_i \partial A_j}\psi_i\psi_j + \text{h.c.}, \quad (44)$$

where ψ and A stand for generic two-component fermion and scalar fields. After spontaneous breaking of the electroweak symmetry, ($\langle H_1^1\rangle = v_1/\sqrt{2}$ and $\langle H_2^2\rangle = v_2/\sqrt{2}$), we have the following set of mass terms written in the four-component spinor notation so that

$$-\mathcal{L}_m = \bar{\xi}_R^T(M_u)\xi_L + \bar{\eta}_R^T(M_d)\eta_L + \text{h.c.}, \tag{45}$$

where the basis vectors are defined in Eq. (3) and Eq. (8).

Next we consider the mixing of the down squarks and the charged mirror sdowns. The mass squared matrix of the sdown - mirror sdown comes from three sources: the F term, the D term of the potential and the soft SUSY breaking terms. Using the superpotential of the mass terms arising from it after the breaking of the electroweak symmetry are given by the Lagrangian

$$\mathcal{L} = \mathcal{L}_F + \mathcal{L}_D + \mathcal{L}_{\text{soft}}\ , \tag{46}$$

where $\mathcal{L}_F$ is deduced from $F_i = \partial W/\partial A_i$, and $-\mathcal{L}_F = V_F = F_i F_i^*$ while the $\mathcal{L}_D$ is given by

$$\begin{aligned}
-\mathcal{L}_D = {} & \frac{1}{2}m_Z^2\cos^2\theta_W\cos 2\beta\{\tilde{t}_L\tilde{t}_L^* - \tilde{b}_L\tilde{b}_L^* + \tilde{c}_L\tilde{c}_L^* - \tilde{s}_L\tilde{s}_L^* + \tilde{u}_L\tilde{u}_L^* - \tilde{d}_L\tilde{d}_L^* + \tilde{t}_{4L}\tilde{t}_{4L}^* - \tilde{b}_{4L}\tilde{b}_{4L}^* \\
& + \tilde{B}_R\tilde{B}_R^* - \tilde{T}_R\tilde{T}_R^*\} + \frac{1}{2}m_Z^2\sin^2\theta_W\cos 2\beta\{-\frac{1}{3}\tilde{t}_L\tilde{t}_L^* + \frac{4}{3}\tilde{t}_R\tilde{t}_R^* - \frac{1}{3}\tilde{c}_L\tilde{c}_L^* + \frac{4}{3}\tilde{c}_R\tilde{c}_R^* \\
& - \frac{1}{3}\tilde{u}_L\tilde{u}_L^* + \frac{4}{3}\tilde{u}_R\tilde{u}_R^* + \frac{1}{3}\tilde{T}_R\tilde{T}_R^* - \frac{4}{3}\tilde{T}_L\tilde{T}_L^* - \frac{1}{3}\tilde{b}_L\tilde{b}_L^* - \frac{2}{3}\tilde{b}_R\tilde{b}_R^* \\
& - \frac{1}{3}\tilde{s}_L\tilde{s}_L^* - \frac{2}{3}\tilde{s}_R\tilde{s}_R^* - \frac{1}{3}\tilde{d}_L\tilde{d}_L^* - \frac{2}{3}\tilde{d}_R\tilde{d}_R^* + \frac{1}{3}\tilde{B}_R\tilde{B}_R^* \\
& + \frac{2}{3}\tilde{B}_L\tilde{B}_L^* - \frac{1}{3}\tilde{t}_{4L}\tilde{t}_{4L}^* + \frac{4}{3}\tilde{t}_{4R}\tilde{t}_{4R}^* - \frac{1}{3}\tilde{b}_{4L}\tilde{b}_{4L}^* - \frac{2}{3}\tilde{b}_{4R}\tilde{b}_{4R}^*\}.
\end{aligned} \tag{47}$$

For $\mathcal{L}_{\text{soft}}$ we assume the following form

$$\begin{aligned}
-\mathcal{L}_{\text{soft}} = {} & M_{\tilde{1}L}^2\tilde{q}_{1L}^{k*}\tilde{q}_{1L}^k + M_{\tilde{4}L}^2\tilde{q}_{4L}^{k*}\tilde{q}_{4L}^k + M_{\tilde{2}L}^2\tilde{q}_{2L}^{k*}\tilde{q}_{2L}^k + M_{\tilde{3}L}^2\tilde{q}_{3L}^{k*}\tilde{q}_{3L}^k + M_{\tilde{Q}}^2\tilde{Q}^{ck*}\tilde{Q}^{ck} + M_{\tilde{t}_1}^2\tilde{t}_{1L}^{c*}\tilde{t}_{1L}^c \\
& + M_{\tilde{b}_1}^2\tilde{b}_{1L}^{c*}\tilde{b}_{1L}^c + M_{\tilde{t}_2}^2\tilde{t}_{2L}^{c*}\tilde{t}_{2L}^c + M_{\tilde{b}_4}^2\tilde{b}_{4L}^{c*}\tilde{b}_{4L}^c + M_{\tilde{t}_4}^2\tilde{t}_{4L}^{c*}\tilde{t}_{4L}^c \\
& + M_{\tilde{t}_3}^2\tilde{t}_{3L}^{c*}\tilde{t}_{3L}^c + M_{\tilde{b}_2}^2\tilde{b}_{2L}^{c*}\tilde{b}_{2L}^c + M_{\tilde{b}_3}^2\tilde{b}_{3L}^{c*}\tilde{b}_{3L}^c + M_{\tilde{B}}^2\tilde{B}_L^*\tilde{B}_L + M_{\tilde{T}}^2\tilde{T}_L^*\tilde{T}_L \\
& + \epsilon_{ij}\{y_1 A_b H_1^i\tilde{q}_{1L}^j\tilde{b}_{1L}^c - y_1' A_t H_2^i\tilde{q}_{1L}^j\tilde{t}_{1L}^c + y_5 A_{4b} H_1^i\tilde{q}_{4L}^j\tilde{b}_{4L}^c - y_5' A_{4t} H_2^i\tilde{q}_{4L}^j\tilde{t}_{4L}^c + y_3 A_s H_1^i\tilde{q}_{2L}^j\tilde{b}_{2L}^c \\
& - y_3' A_c H_2^i\tilde{q}_{2L}^j\tilde{t}_{2L}^c + y_4 A_d H_1^i\tilde{q}_{3L}^j\tilde{b}_{3L}^c - y_4' A_u H_2^i\tilde{q}_{3L}^j\tilde{t}_{3L}^c + y_2 A_T H_1^i\tilde{Q}^{cj}\tilde{T}_L - y_2' A_B H_2^i\tilde{Q}^{cj}\tilde{B}_L + \text{h.c.}\}\ .
\end{aligned} \tag{48}$$

Here $M_{\tilde{1}L}, M_{\tilde{T}}$, etc are the soft masses and A_t, A_b, etc are the trilinear couplings. The trilinear couplings are complex and we define their phases so that

$$A_b = |A_b|e^{i\alpha_{A_b}}\ ,\quad A_t = |A_t|e^{i\alpha_{A_t}}\ ,\cdots\ . \tag{49}$$

From these terms we construct the scalar mass squared matrices. Thus we define the scalar mass squared matrix $M^2_{\tilde{d}}$ in the basis $(\tilde{b}_L, \tilde{B}_L, \tilde{b}_R, \tilde{B}_R, \tilde{s}_L, \tilde{s}_R, \tilde{d}_L, \tilde{d}_R, \tilde{b}_{4L}, \tilde{b}_{4R})$. We label the matrix elements of these as $(M^2_{\tilde{d}})_{ij} = M^2_{ij}$ which is a hermitian matrix. We can diagonalize this hermitian mass squared matrix by the unitary transformation

$$\tilde{D}^{d\dagger} M^2_{\tilde{d}} \tilde{D}^d = diag(M^2_{\tilde{d}_1}, M^2_{\tilde{d}_2}, M^2_{\tilde{d}_3}, M^2_{\tilde{d}_4}, M^2_{\tilde{d}_5}, M^2_{\tilde{d}_6}, M^2_{\tilde{d}_7}, M^2_{\tilde{d}_8} M^2_{\tilde{d}_9}, M^2_{\tilde{d}_{10}}) \ . \tag{50}$$

Similarly we write the mass squared matrix in the up squark sector in the basis $(\tilde{t}_L, \tilde{T}_L, \tilde{t}_R, \tilde{T}_R, \tilde{c}_L, \tilde{c}_R, \tilde{u}_L, \tilde{u}_R, \tilde{t}_{4L}, \tilde{t}_{4R})$. Thus here we denote the up squark mass squared matrix in the form $(M^2_{\tilde{u}})_{ij} = m^2_{ij}$ which is also a hermitian matrix. We can diagonalize this mass square matrix by the unitary transformation

$$\tilde{D}^{u\dagger} M^2_{\tilde{u}} \tilde{D}^u = \mathrm{diag}(M^2_{\tilde{u}_1}, M^2_{\tilde{u}_2}, M^2_{\tilde{u}_3}, M^2_{\tilde{u}_4}, M^2_{\tilde{u}_5}, M^2_{\tilde{u}_6}, M^2_{\tilde{u}_7}, M^2_{\tilde{u}_8}, M^2_{\tilde{u}_9}, M^2_{\tilde{u}_{10}}) \ . \tag{51}$$

8 Appendix B: W, Z, $\tilde{\chi}^{\pm}$, $\tilde{\chi}^0$, $\tilde{g}$ couplings with quarks

8.1 W-quark -quark couplings

The couplings that enter in the W -quark -squark interactions of Eq. (13) are defined so that

$$G^W_{L_{ji}} = \frac{g}{\sqrt{2}}[D^{u*}_{L5j} D^d_{L5i} + D^{u*}_{L4j} D^d_{L4i} + D^{u*}_{L3j} D^d_{L3i} + D^{u*}_{L1j} D^d_{L1i}], \tag{52}$$

$$G^W_{R_{ji}} = \frac{g}{\sqrt{2}}[D^{u*}_{R2j} D^d_{R2i}]. \tag{53}$$

8.2 Z-quark -quark couplings

The couplings that enter in the Z -up-quark interactions of Eq. (18) are defined so that

$$C^{uZ}_{L_{ji}} = \frac{g}{\cos\theta_W}[x_1(D^{u*}_{L5j} D^u_{L5i} + D^{u*}_{L4j} D^u_{L4i} + D^{u*}_{L1j} D^u_{L1i} + D^{u*}_{L3j} D^u_{L3i}) + y_1 D^{u*}_{L2j} D^u_{L2i}], \tag{54}$$

and

$$C^{uZ}_{R_{ji}} = \frac{g}{\cos\theta_W}[y_1(D^{u*}_{R5j} D^u_{R5i} + D^{u*}_{R4j} D^u_{R4i} + D^{u*}_{R1j} D^u_{R1i} + D^{u*}_{R3j} D^u_{R3i}) + x_1 D^{u*}_{R2j} D^u_{R2i}], \tag{55}$$

where

$$x_1 = \frac{1}{2} - \frac{2}{3}\sin^2\theta_W, \quad y_1 = -\frac{2}{3}\sin^2\theta_W. \tag{56}$$

The couplings that enter in the Z-down-quark interactions of Eq. (20) are defined so that

$$C^{dZ}_{L_{ji}} = \frac{g}{\cos\theta_W}[x_2(D^{d*}_{L5j}D^d_{L5i} + D^{d*}_{L4j}D^d_{L4i} + D^{d*}_{L1j}D^d_{L1i} + D^{d*}_{L3j}D^d_{L3i}) + y_2 D^{d*}_{L2j}D^d_{L2i}], \tag{57}$$

and

$$C^{dZ}_{R_{ji}} = \frac{g}{\cos\theta_W}[y_2(D^{d*}_{R5j}D^d_{R5i} + D^{d*}_{R4j}D^d_{R4i} + D^{d*}_{R1j}D^d_{R1i} + D^{d*}_{R3j}D^d_{R3i}) + x_2 D^{d*}_{R2j}D^d_{R2i}], \tag{58}$$

where

$$x_2 = -\frac{1}{2} + \frac{1}{3}\sin^2\theta_W, \quad y_2 = \frac{1}{3}\sin^2\theta_W. \tag{59}$$

8.3 Chargino-quark-squark couplings

The couplings that enter in the chargino-up-quark-down-squark interactions of Eq. (23) are given by

$$\begin{aligned} C^{Lu}_{jik} =& g(-\kappa_u V^*_{i2} D^{u*}_{R4j}\tilde{D}^d_{7k} - \kappa_c V^*_{i2} D^{u*}_{R3j}\tilde{D}^d_{5k} \\ & - \kappa_t V^*_{i2} D^{u*}_{R1j}\tilde{D}^d_{1k} - \kappa_{4t} V^*_{i2} D^{u*}_{R5j}\tilde{D}^d_{9k} - \kappa_B V^*_{i2} D^{u*}_{R2j}\tilde{D}^d_{2k} + V^*_{i1} D^{u*}_{R2j}\tilde{D}^d_{4k}), \end{aligned} \tag{60}$$

$$\begin{aligned} C^{Ru}_{jik} =& g(-\kappa_d U_{i2} D^{u*}_{L4j}\tilde{D}^d_{8k} - \kappa_s U_{i2} D^{u*}_{L3j}\tilde{D}^d_{6k} - \kappa_b U_{i2} D^{u*}_{L1j}\tilde{D}^d_{3k} \\ & - \kappa_{4b} U_{i2} D^{u*}_{L5j}\tilde{D}^d_{10k} - \kappa_T U_{i2} D^{u*}_{L2j}\tilde{D}^d_{4k} \\ & + U_{i1} D^{u*}_{L4j}\tilde{D}^d_{7k} + U_{i1} D^{u*}_{L3j}\tilde{D}^d_{5k} + U_{i1} D^{u*}_{L1j}\tilde{D}^d_{1k} + U_{i1} D^{u*}_{L5j}\tilde{D}^d_{9k}), \end{aligned} \tag{61}$$

The couplings that enter in the chargino-down-quark-up-squark interactions of Eq. (22) are given by

$$\begin{aligned} C^{Ld}_{jik} =& g(-\kappa_d U^*_{i2} D^{d*}_{R4j}\tilde{D}^u_{7k} - \kappa_s U^*_{i2} D^{d*}_{R3j}\tilde{D}^u_{5k} \\ & - \kappa_b U^*_{i2} D^{d*}_{R1j}\tilde{D}^u_{1k} - \kappa_{4b} U^*_{i2} D^{d*}_{R5j}\tilde{D}^u_{9k} - \kappa_T U^*_{i2} D^{d*}_{R2j}\tilde{D}^u_{2k} + U^*_{i1} D^{d*}_{R2j}\tilde{D}^u_{4k}), \end{aligned} \tag{62}$$

$$\begin{aligned} C^{Rd}_{jik} =& g(-\kappa_u V_{i2} D^{d*}_{L4j}\tilde{D}^u_{8k} - \kappa_c V_{i2} D^{d*}_{L3j}\tilde{D}^u_{6k} - \kappa_t V_{i2} D^{d*}_{L1j}\tilde{D}^u_{3k} - \kappa_{4t} V_{i2} D^{d*}_{L5j}\tilde{D}^u_{10k} \\ & - \kappa_B V_{i2} D^{d*}_{L2j}\tilde{D}^u_{4k} + V_{i1} D^{d*}_{L4j}\tilde{D}^u_{7k} + V_{i1} D^{d*}_{L3j}\tilde{D}^u_{5k} + V_{i1} D^{d*}_{L1j}\tilde{D}^u_{1k} + V_{i1} D^{d*}_{L5j}\tilde{D}^u_{9k}), \end{aligned} \tag{63}$$

where

$$(\kappa_T, \kappa_b, \kappa_s, \kappa_d, \kappa_{4b}) = \frac{(m_T, m_b, m_s, m_d, m_{4b})}{\sqrt{2} m_W \cos\beta}, \tag{64}$$

$$(\kappa_B, \kappa_t, \kappa_c, \kappa_u, \kappa_{4t}) = \frac{(m_B, m_t, m_c, m_u, m_{4t})}{\sqrt{2} m_W \sin\beta}. \tag{65}$$

and

$$U^* M_C V = \mathrm{diag}(m_{\tilde{\chi}_1^-}, m_{\tilde{\chi}_2^-}). \tag{66}$$

8.4 Neutralino-quark-squark couplings

We first give the discuss the couplings that enter the the interactions in the mass diagonal basis involving up quarks, up squarks and neutralinos of Eq. (28). Here we have,

$$\begin{aligned} C'^{L}_{uijk} =& \sqrt{2}(\alpha_{uj} D^{u*}_{R4i} \tilde{D}^{u}_{7k} - \gamma_{uj} D^{u*}_{R4i} \tilde{D}^{u}_{8k} + \alpha_{cj} D^{u*}_{R3i} \tilde{D}^{u}_{5k} - \gamma_{cj} D^{u*}_{R3i} \tilde{D}^{u}_{6k} + \alpha_{tj} D^{u*}_{R1i} \tilde{D}^{u}_{1k} \\ &- \gamma_{tj} D^{u*}_{R1i} \tilde{D}^{u}_{3k} + \alpha_{4tj} D^{u*}_{R5i} \tilde{D}^{u}_{9k} - \gamma_{4tj} D^{u*}_{R5i} \tilde{D}^{u}_{10k} + \beta_{Tj} D^{u*}_{R2i} \tilde{D}^{u}_{4k} - \delta_{Tj} D^{u*}_{R2i} \tilde{D}^{u}_{2k}), \end{aligned} \tag{67}$$

$$\begin{aligned} C'^{R}_{uijk} =& \sqrt{2}(\beta_{uj} D^{u*}_{L4i} \tilde{D}^{u}_{7k} - \delta_{uj} D^{u*}_{L4i} \tilde{D}^{u}_{8k} + \beta_{cj} D^{u*}_{L3i} \tilde{D}^{u}_{5k} - \delta_{cj} D^{u*}_{L3i} \tilde{D}^{u}_{6k} + \beta_{tj} D^{u*}_{L1i} \tilde{D}^{u}_{1k} \\ &- \delta_{tj} D^{u*}_{L1i} \tilde{D}^{u}_{3k} + \beta_{4tj} D^{u*}_{L5i} \tilde{D}^{u}_{9k} - \delta_{4tj} D^{u*}_{L5i} \tilde{D}^{u}_{10k} + \alpha_{Tj} D^{u*}_{L2i} \tilde{D}^{u}_{4k} - \gamma_{Tj} D^{u*}_{L2i} \tilde{D}^{u}_{2k}), \end{aligned} \tag{68}$$

where

$$\alpha_{Tj} = \frac{g m_T X^*_{3j}}{2 m_W \cos\beta} ; \qquad \beta_{Tj} = -\frac{2}{3} e X'_{1j} + \frac{g}{\cos\theta_W} X'_{2j} \left(-\frac{1}{2} + \frac{2}{3}\sin^2\theta_W\right) \tag{69}$$

$$\gamma_{Tj} = -\frac{2}{3} e X'^{*}_{1j} + \frac{2}{3} \frac{g \sin^2\theta_W}{\cos\theta_W} X'^{*}_{2j} ; \quad \delta_{Tj} = -\frac{g m_T X_{3j}}{2 m_W \cos\beta} \tag{70}$$

and

$$\alpha_{4tj} = \frac{g m_{4t} X_{4j}}{2 m_W \sin\beta} ; \quad \alpha_{tj} = \frac{g m_t X_{4j}}{2 m_W \sin\beta} ; \quad \alpha_{cj} = \frac{g m_c X_{4j}}{2 m_W \sin\beta} ; \quad \alpha_{uj} = \frac{g m_u X_{4j}}{2 m_W \sin\beta} \tag{71}$$

$$\delta_{4tj} = -\frac{g m_{4t} X^*_{4j}}{2 m_W \sin\beta} ; \quad \delta_{tj} = -\frac{g m_t X^*_{4j}}{2 m_W \sin\beta} ; \quad \delta_{cj} = -\frac{g m_c X^*_{4j}}{2 m_W \sin\beta} ; \quad \delta_{uj} = -\frac{g m_u X^*_{4j}}{2 m_W \sin\beta} \tag{72}$$

and where

$$\beta_{4tj} = \beta_{tj} = \beta_{cj} = \beta_{uj} = \frac{2}{3} e X'^{*}_{1j} + \frac{g}{\cos\theta_W} X'^{*}_{2j} \left(\frac{1}{2} - \frac{2}{3}\sin^2\theta_W\right) \tag{73}$$

$$\gamma_{4tj} = \gamma_{tj} = \gamma_{cj} = \gamma_{uj} = \frac{2}{3} e X'_{1j} - \frac{2}{3} \frac{g \sin^2\theta_W}{\cos\theta_W} X'_{2j} \tag{74}$$

Similarly for the couplings that enter the the interactions in the mass diagonal basis involving down quarks, down squarks and neutralinos of Eq. (29) we have

$$\begin{aligned} C'^{L}_{dijk} =&\sqrt{2}(\alpha_{dj} D^{d*}_{R4i}\tilde{D}^{d}_{7k} - \gamma_{dj} D^{d*}_{R4i}\tilde{D}^{d}_{8k} + \alpha_{sj} D^{d*}_{R3i}\tilde{D}^{d}_{5k} - \gamma_{sj} D^{d*}_{R3i}\tilde{D}^{d}_{6k} + \alpha_{bj} D^{d*}_{R1i}\tilde{D}^{d}_{1k} - \gamma_{bj} D^{d*}_{R1i}\tilde{D}^{d}_{3k} \\ &+ \alpha_{4bj} D^{d*}_{R5i}\tilde{D}^{d}_{9k} - \gamma_{4bj} D^{d*}_{R5i}\tilde{D}^{d}_{10k} + \beta_{Bj} D^{d*}_{R2i}\tilde{D}^{d}_{4k} - \delta_{Bj} D^{d*}_{R2i}\tilde{D}^{d}_{2k}), \end{aligned} \tag{75}$$

and

$$\begin{aligned} C'^{R}_{dijk} =&\sqrt{2}(\beta_{dj} D^{d*}_{L4i}\tilde{D}^{d}_{7k} - \delta_{dj} D^{d*}_{L4i}\tilde{D}^{d}_{8k} + \beta_{sj} D^{d*}_{L3i}\tilde{D}^{d}_{5k} - \delta_{sj} D^{d*}_{L3i}\tilde{D}^{d}_{6k} + \beta_{bj} D^{d*}_{L1i}\tilde{D}^{d}_{1k} - \delta_{bj} D^{d*}_{L1i}\tilde{D}^{d}_{3k} \\ &+ \beta_{4bj} D^{d*}_{L5i}\tilde{D}^{d}_{9k} - \delta_{4bj} D^{d*}_{L5i}\tilde{D}^{d}_{10k} + \alpha_{Bj} D^{d*}_{L2i}\tilde{D}^{d}_{4k} - \gamma_{Bj} D^{d*}_{L2i}\tilde{D}^{d}_{2k}), \end{aligned} \tag{76}$$

where

$$\alpha_{Bj} = \frac{g m_B X^*_{4j}}{2 m_W \sin\beta} \; ; \qquad \beta_{Bj} = \frac{1}{3} e X'_{1j} + \frac{g}{\cos\theta_W} X'_{2j} \left(\frac{1}{2} - \frac{1}{3}\sin^2\theta_W\right) \tag{77}$$

$$\gamma_{Bj} = \frac{1}{3} e X'^*_{1j} - \frac{1}{3}\frac{g \sin^2\theta_W}{\cos\theta_W} X'^*_{2j} \; ; \qquad \delta_{Bj} = -\frac{g m_B X_{4j}}{2 m_W \sin\beta} \tag{78}$$

and

$$\alpha_{4bj} = \frac{g m_{4b} X_{3j}}{2 m_W \cos\beta} \; ; \quad \alpha_{bj} = \frac{g m_b X_{3j}}{2 m_W \cos\beta} \; ; \quad \alpha_{sj} = \frac{g m_s X_{3j}}{2 m_W \cos\beta} \; ; \quad \alpha_{dj} = \frac{g m_d X_{3j}}{2 m_W \cos\beta} \tag{79}$$

$$\delta_{4bj} = -\frac{g m_{4b} X^*_{3j}}{2 m_W \cos\beta} \; ; \quad \delta_{bj} = -\frac{g m_b X^*_{3j}}{2 m_W \cos\beta} \; ; \quad \delta_{sj} = -\frac{g m_s X^*_{3j}}{2 m_W \cos\beta} \; ; \quad \delta_{dj} = -\frac{g m_d X^*_{3j}}{2 m_W \cos\beta} \tag{80}$$

and where

$$\beta_{4bj} = \beta_{bj} = \beta_{sj} = \beta_{dj} = -\frac{1}{3} e X'^*_{1j} + \frac{g}{\cos\theta_W} X'^*_{2j} \left(-\frac{1}{2} + \frac{1}{3}\sin^2\theta_W\right) \tag{81}$$

$$\gamma_{4bj} = \gamma_{bj} = \gamma_{sj} = \gamma_{dj} = -\frac{1}{3} e X'_{1j} + \frac{1}{3}\frac{g \sin^2\theta_W}{\cos\theta_W} X'_{2j} \tag{82}$$

Here X' are defined by

$$X'_{1i} = X_{1i}\cos\theta_W + X_{2i}\sin\theta_W \tag{83}$$

$$X'_{2i} = -X_{1i}\sin\theta_W + X_{2i}\cos\theta_W, \tag{84}$$

where X diagonalizes the neutralino mass matrix and is defined by

$$X^T M_{\chi^0} X = \mathrm{diag}\left(m_{\tilde{\chi}_1^0}, m_{\tilde{\chi}_2^0}, m_{\tilde{\chi}_3^0}, m_{\tilde{\chi}_4^0}\right). \tag{85}$$

8.5 Gluino-quark-squark-couplings

The couplings that enter in the gluino-quark-squark interactions of Eq. (32) are given by

$$C_{L_{lm}} = (D^{q*}_{R2l}\tilde{D}^q_{4m} - D^{q*}_{R5l}\tilde{D}^q_{10m} - D^{q*}_{R4l}\tilde{D}^q_{8m} - D^{q*}_{R3l}\tilde{D}^q_{6m} - D^{q*}_{R1l}\tilde{D}^q_{3m})e^{-i\xi_3/2}, \tag{86}$$

and

$$C_{R_{lm}} = (D^{q*}_{L4l}\tilde{D}^q_{7m} + D^{q*}_{L5l}\tilde{D}^q_{9m} + D^{q*}_{L3l}\tilde{D}^q_{5m} + D^{q*}_{L1l}\tilde{D}^q_{1m} - D^{q*}_{L2l}\tilde{D}^q_{2m})e^{i\xi_3/2}, \tag{87}$$

where ξ_3 is the phase of the gluino mass.

9 Appendix: Mass squared matrices for the scalars

We define the scalar mass squared matrix $M^2_{\tilde{d}}$ in the basis $(\tilde{b}_L, \tilde{B}_L, \tilde{b}_R, \tilde{B}_R, \tilde{s}_L, \tilde{s}_R, \tilde{d}_L, \tilde{d}_R, \tilde{b}_{4L}, \tilde{b}_{4R})$. We label the matrix elements of these as $(M^2_{\tilde{d}})_{ij} = M^2_{ij}$ where the elements of the matrix are given by

$$\begin{aligned}
M^2_{11} &= M^2_{\tilde{1}L} + \frac{v_1^2|y_1|^2}{2} + |h_3|^2 - m_Z^2\cos 2\beta\left(\frac{1}{2} - \frac{1}{3}\sin^2\theta_W\right),\\
M^2_{22} &= M^2_{\tilde{B}} + \frac{v_2^2|y_2'|^2}{2} + |h_4|^2 + |h_4'|^2 + |h_4''|^2 + |h_7|^2 + \frac{1}{3}m_Z^2\cos 2\beta\sin^2\theta_W,\\
M^2_{33} &= M^2_{\tilde{b}_1} + \frac{v_1^2|y_1|^2}{2} + |h_4|^2 - \frac{1}{3}m_Z^2\cos 2\beta\sin^2\theta_W,\\
M^2_{44} &= M^2_{\tilde{Q}} + \frac{v_2^2|y_2'|^2}{2} + |h_3|^2 + |h_3'|^2 + |h_3''|^2 + |h_6|^2 + m_Z^2\cos 2\beta\left(\frac{1}{2} - \frac{1}{3}\sin^2\theta_W\right),
\end{aligned}$$

$$
\begin{aligned}
M_{55}^2 &= M_{\tilde{2}L}^2 + \frac{v_1^2|y_3|^2}{2} + |h_3'|^2 - m_Z^2 \cos 2\beta \left(\frac{1}{2} - \frac{1}{3}\sin^2\theta_W\right), \\
M_{66}^2 &= M_{\tilde{b}_2}^2 + \frac{v_1^2|y_3|^2}{2} + |h_4'|^2 - \frac{1}{3} m_Z^2 \cos 2\beta \sin^2\theta_W, \\
M_{77}^2 &= M_{\tilde{3}L}^2 + \frac{v_1^2|y_4|^2}{2} + |h_3''|^2 - m_Z^2 \cos 2\beta \left(\frac{1}{2} - \frac{1}{3}\sin^2\theta_W\right), \\
M_{88}^2 &= M_{\tilde{b}_3}^2 + \frac{v_1^2|y_4|^2}{2} + |h_4''|^2 - \frac{1}{3} m_Z^2 \cos 2\beta \sin^2\theta_W\ . \\
M_{99}^2 &= M_{\tilde{4}L}^2 + \frac{v_1^2|y_5|^2}{2} + |h_6|^2 - m_Z^2 \cos 2\beta \left(\frac{1}{2} - \frac{1}{3}\sin^2\theta_W\right) \\
M_{1010}^2 &= M_{\tilde{b}_4}^2 + \frac{v_1^2|y_5|^2}{2} + |h_7|^2 - \frac{1}{3} m_Z^2 \cos 2\beta \sin^2\theta_W\ .
\end{aligned}
\tag{88}
$$

$$M^2_{12}=M^{2*}_{21}=\frac{v_2y_2'h_3^*}{\sqrt{2}}+\frac{v_1h_4y_1^*}{\sqrt{2}}, M^2_{13}=M^{2*}_{31}=\frac{y_1^*}{\sqrt{2}}(v_1A_b^*-\mu v_2), M^2_{14}=M^{2*}_{41}=0,$$
$$M^2_{15}=M^{2*}_{51}=h_3'h_3^*, M^2_{16}=M^{2*}_{61}=0, M^2_{17}=M^{2*}_{71}=h_3''h_3^*, M^2_{18}=M^{2*}_{81}=0, M^2_{19}=M^{2*}_{91}=h_3^*h_6,$$
$$M^2_{110}=M^{2*}_{101}=0, M^2_{23}=M^{2*}_{32}=0, M^2_{24}=M^{2*}_{42}=\frac{y_2'^*}{\sqrt{2}}(v_2A_B^*-\mu v_1), M^2_{25}=M^{2*}_{52}=\frac{v_2h_3'y_2'^*}{\sqrt{2}}+\frac{v_1y_3h_4^*}{\sqrt{2}},$$
$$M^2_{26}=M^{2*}_{62}=0, M^2_{27}=M^{2*}_{72}=\frac{v_2h_3''y_2'^*}{\sqrt{2}}+\frac{v_1y_4h_4''^*}{\sqrt{2}}, M^2_{28}=M^{2*}_{82}=0,$$
$$M^2_{29}=M^{2*}_{92}=\frac{v_1h_7^*y_5}{\sqrt{2}}+\frac{v_2y_2'^*h_6}{\sqrt{2}}, M^2_{210}=M^{2*}_{102}=0,$$
$$M^2_{34}=M^{2*}_{43}=\frac{v_2h_4y_2'^*}{\sqrt{2}}+\frac{v_1y_1h_3^*}{\sqrt{2}}, M^2_{35}=M^{2*}_{53}=0, M^2_{36}=M^{2*}_{63}=h_4h_4'^*,$$
$$M^2_{37}=M^{2*}_{73}=0, M^2_{38}=M^{2*}_{83}=h_4h_4''^*,$$
$$M^2_{39}=M^{2*}_{93}=0, M^2_{310}=M^{2*}_{103}=h_4h_7^*,$$
$$M^2_{45}=M^{2*}_{54}=0, M^2_{46}=M^{2*}_{64}=\frac{v_2y_2'h_4'^*}{\sqrt{2}}+\frac{v_1h_3'y_3^*}{\sqrt{2}},$$
$$M^2_{47}=M^{2*}_{74}=0, M^2_{48}=M^{2*}_{84}=\frac{v_2y_2'h_4''^*}{\sqrt{2}}+\frac{v_1h_3''y_4^*}{\sqrt{2}},$$
$$M^2_{49}=M^{2*}_{94}=0, M^2_{410}=M^{2*}_{104}=\frac{v_2y_2'h_7^*}{\sqrt{2}}+\frac{v_1h_6y_5^*}{\sqrt{2}},$$
$$M^2_{56}=M^{2*}_{65}=\frac{y_3^*}{\sqrt{2}}(v_1A_s^*-\mu v_2), M^2_{57}=M^{2*}_{75}=h_3''h_3'^*,$$
$$M^2_{58}=M^{2*}_{85}=0, M^2_{59}=M^{2*}_{95}=h_3'^*h_6, M^2_{510}=M^{2*}_{105}=0, M^2_{67}=M^{2*}_{76}=0,$$
$$M^2_{68}=M^{2*}_{86}=h_4'h_4''^*, M^2_{69}=M^{2*}_{96}=0, M^2_{610}=M^{2*}_{106}=h_4'h_7^*, M^2_{78}=M^{2*}_{87}=\frac{y_4^*}{\sqrt{2}}(v_1A_d^*-\mu v_2)\ .$$
$$M^2_{79}=M^{2*}_{97}=h_3''^*h_6, M^2_{710}=M^{2*}_{107}=0$$
$$M^2_{89}=M^{2*}_{98}=0, M^2_{810}=M^{2*}_{108}=h_4''h_7^*, M^2_{910}=M^{2*}_{109}=\frac{y_5^*}{\sqrt{2}}(v_1A_{4b}^*-\mu v_2)\ .$$

We can diagonalize this hermitian mass squared matrix by the unitary transformation

$$\tilde{D}^{d\dagger}M^2_{\tilde{d}}\tilde{D}^d=diag(M^2_{\tilde{d}_1},M^2_{\tilde{d}_2},M^2_{\tilde{d}_3},M^2_{\tilde{d}_4},M^2_{\tilde{d}_5},M^2_{\tilde{d}_6},M^2_{\tilde{d}_7},M^2_{\tilde{d}_8},M^2_{\tilde{d}_9},M^2_{\tilde{d}_{10}})\ . \qquad (89)$$

Next we write the mass^2 matrix in the sups sector the basis $(\tilde{t}_L,\tilde{T}_L,\tilde{t}_R,\tilde{T}_R,\tilde{c}_L,\tilde{c}_R,\tilde{u}_L,\tilde{u}_R,\tilde{t}_{4L},\tilde{t}_{4R})$. Thus here we denote the sups mass^2 matrix in the form $(M^2_{\tilde{u}})_{ij}=m^2_{ij}$ where

$$m_{11}^2 = M_{\tilde{1}L}^2 + \frac{v_2^2|y_1'|^2}{2} + |h_3|^2 + m_Z^2 \cos 2\beta \left(\frac{1}{2} - \frac{2}{3}\sin^2\theta_W\right),$$
$$m_{22}^2 = M_{\tilde{T}}^2 + \frac{v_1^2|y_2|^2}{2} + |h_5|^2 + |h_5'|^2 + |h_5''|^2 + |h_8|^2 - \frac{2}{3}m_Z^2 \cos 2\beta \sin^2\theta_W,$$
$$m_{33}^2 = M_{\tilde{t}_1}^2 + \frac{v_2^2|y_1'|^2}{2} + |h_5|^2 + \frac{2}{3}m_Z^2 \cos 2\beta \sin^2\theta_W,$$
$$m_{44}^2 = M_{\tilde{Q}}^2 + \frac{v_1^2|y_2|^2}{2} + |h_3|^2 + |h_3'|^2 + |h_3''|^2 + |h_6|^2 - m_Z^2 \cos 2\beta \left(\frac{1}{2} - \frac{2}{3}\sin^2\theta_W\right),$$

$$m_{55}^2 = M_{\tilde{2}L}^2 + \frac{v_2^2|y_3'|^2}{2} + |h_3'|^2 + m_Z^2 \cos 2\beta \left(\frac{1}{2} - \frac{2}{3}\sin^2\theta_W\right),$$
$$m_{66}^2 = M_{\tilde{t}_2}^2 + \frac{v_2^2|y_3'|^2}{2} + |h_5'|^2 + \frac{2}{3}m_Z^2 \cos 2\beta \sin^2\theta_W,$$
$$m_{77}^2 = M_{\tilde{3}L}^2 + \frac{v_2^2|y_4'|^2}{2} + |h_3''|^2 + m_Z^2 \cos 2\beta \left(\frac{1}{2} - \frac{2}{3}\sin^2\theta_W\right),$$
$$m_{88}^2 = M_{\tilde{t}_3}^2 + \frac{v_2^2|y_4'|^2}{2} + |h_5''|^2 + \frac{2}{3}m_Z^2 \cos 2\beta \sin^2\theta_W,$$
$$m_{99}^2 = M_{\tilde{4}L}^2 + \frac{v_2^2|y_5'|^2}{2} + |h_6|^2 + m_Z^2 \cos 2\beta \left(\frac{1}{2} - \frac{2}{3}\sin^2\theta_W\right),$$
$$m_{1010}^2 = M_{\tilde{t}_4}^2 + \frac{v_2^2|y_5'|^2}{2} + |h_8|^2 + \frac{2}{3}m_Z^2 \cos 2\beta \sin^2\theta_W.$$

$$
\begin{aligned}
&m_{12}^2 = m_{21}^{2*} = -\frac{v_1 y_2 h_3^*}{\sqrt{2}} + \frac{v_2 h_5 y_1'^*}{\sqrt{2}}, m_{13}^2 = m_{31}^{2*} = \frac{y_1'^*}{\sqrt{2}}(v_2 A_t^* - \mu v_1), m_{14}^2 = m_{41}^{2*} = 0,\\
&m_{15}^2 = m_{51}^{2*} = h_3' h_3^*, m_{16}^2 = m_{61}^{2*} = 0, m_{17}^2 = m_{71}^{2*} = h_3'' h_3^*, m_{18}^2 = m_{81}^{2*} = 0,\\
&m_{23}^2 = m_{32}^{2*} = 0, m_{24}^2 = m_{42}^{2*} = \frac{y_2^*}{\sqrt{2}}(v_1 A_T^* - \mu v_2), m_{25}^2 = m_{52}^{2*} = -\frac{v_1 h_3' y_2^*}{\sqrt{2}} + \frac{v_2 y_3' h_5'^*}{\sqrt{2}},\\
&m_{26}^2 = m_{62}^{2*} = 0, m_{27}^2 = m_{72}^{2*} = -\frac{v_1 h_3'' y_2^*}{\sqrt{2}} + \frac{v_2 y_4' h_5''^*}{\sqrt{2}}, m_{28}^2 = m_{82}^{2*} = 0,\\
&m_{34}^2 = m_{43}^{2*} = \frac{v_1 h_5 y_2^*}{\sqrt{2}} - \frac{v_2 y_1' h_3^*}{\sqrt{2}}, m_{35}^2 = m_{53}^{2*} = 0, m_{36}^2 = m_{63}^{2*} = h_5 h_5'^*,\\
&m_{37}^2 = m_{73}^{2*} = 0, m_{38}^2 = m_{83}^{2*} = h_5 h_5''^*,\\
&m_{45}^2 = m_{54}^{2*} = 0, m_{46}^2 = m_{64}^{2*} = -\frac{y_3'^* v_2 h_3'}{\sqrt{2}} + \frac{v_1 y_2 h_5'^*}{\sqrt{2}},\\
&m_{47}^2 = m_{74}^{2*} = 0, m_{48}^2 = m_{84}^{2*} = \frac{v_1 y_2 h_5''^*}{\sqrt{2}} - \frac{v_2 y_4'^* h_3''}{\sqrt{2}},\\
&m_{56}^2 = m_{65}^{2*} = \frac{y_3'^*}{\sqrt{2}}(v_2 A_c^* - \mu v_1),\\
&m_{57}^2 = m_{75}^{2*} = h_3'' h_3'^*, m_{58}^2 = m_{85}^{2*} = 0,\\
&m_{67}^2 = m_{76}^{2*} = 0, m_{68}^2 = m_{86}^{2*} = h_5' h_5''^*,\\
&m_{78}^2 = m_{87}^{2*} = \frac{y_4'^*}{\sqrt{2}}(v_2 A_u^* - \mu v_1),\\
&m_{19}^2 = m_{91}^{2*} = h_6 h_3^*, m_{110}^2 = m_{101}^{2*} = 0,\\
&m_{29}^2 = m_{92}^{2*} = -\frac{y_2^* v_1 h_6}{\sqrt{2}} + \frac{v_2 y_5^* h_8}{\sqrt{2}},\\
&m_{210}^2 = m_{102}^{2*} = 0, m_{39}^2 = m_{93}^{2*} = 0,\\
&m_{310}^2 = m_{103}^{2*} = h_5 h_8^*,\\
&m_{49}^2 = m_{94}^{2*} = 0, m_{410}^2 = m_{104}^{2*} = -\frac{y_5'^* v_2 h_6}{\sqrt{2}} + \frac{v_1 y_2 h_8^*}{\sqrt{2}},\\
&m_{59}^2 = m_{95}^{2*} = h_6 h_3'^*, m_{510}^2 = m_{105}^{2*} = 0\\
&m_{69}^2 = m_{96}^{2*} = 0, m_{610}^2 = m_{106}^{2*} = h_5' h_8^*\\
&m_{79}^2 = m_{97}^{2*} = h_6 h_3''^*, m_{710}^2 = m_{107}^{2*} = 0,\\
&m_{89}^2 = m_{98}^{2*} = 0, m_{810}^2 = m_{108}^{2*} = h_5'' h_8^*,\\
&m_{910}^2 = m_{109}^{2*} = \frac{y_5'^*}{\sqrt{2}}(v_2 A_{4t}^* - \mu v_1) \qquad (90)
\end{aligned}
$$

We can diagonalize the sneutrino mass square matrix by the unitary transformation

$$\tilde{D}^{u\dagger} M_{\tilde{u}}^2 \tilde{D}^u = \mathrm{diag}(M_{\tilde{u}_1}^2, M_{\tilde{u}_2}^2, M_{\tilde{u}_3}^2, M_{\tilde{u}_4}^2, M_{\tilde{u}_5}^2, M_{\tilde{u}_6}^2, M_{\tilde{u}_7}^2, M_{\tilde{u}_8}^2 M_{\tilde{u}_9}^2, M_{\tilde{u}_{10}}^2) \ . \tag{91}$$

References

[1] R. Golub and K. Lamoreaux, Phys. Rept. **237**, 1 (1994).

[2] W. Bernreuther and M. Suzuki, Rev. Mod. Phys. 63, 313 (1991); I.I.Y. Bigi and N. G. Uraltsev, Sov. Phys. JETP 73, 198 (1991); M. J. Booth, eprint hep-ph/9301293; Gavela, M. B., et al., Phys. Lett. B109, 215 (1982); I. B. Khriplovich and A. R. Zhitnitsky, Phys. Lett. B109, 490 (1982); E. P. Shabalin, Sov. Phys. Usp. 26, 297 (1983); I. B. Kriplovich and S. K. Lamoureaux, *CP Violation Without Strangeness*, (Springer, 1997).

[3] T. Ibrahim and P. Nath, Rev. Mod. Phys. **80**, 577 (2008); arXiv:hep-ph/0210251. A. Pilaftsis, hep-ph/9908373; M. Pospelov and A. Ritz, Annals Phys. **318**, 119 (2005) [hep-ph/0504231]; J. Engel, M. J. Ramsey-Musolf and U. van Kolck, Prog. Part. Nucl. Phys. **71**, 21 (2013) [arXiv:1303.2371 [nucl-th]].

[4] J. L. Hewett, H. Weerts, R. Brock, J. N. Butler, B. C. K. Casey, J. Collar, A. de Gouvea and R. Essig *et al.*, arXiv:1205.2671 [hep-ex].

[5] F. Hoogeveen, Nucl. Phys. B **341**, 322 (1990).

[6] A. Soni and R. M. Xu, Phys. Rev. Lett. **69**, 33 (1992).

[7] The analysis of [5] was for the electron and other EDMs are obtained by scaling as noted in [6].

[8] H. Georgi, Nucl. Phys. B **156**, 126 (1979); F. Wilczek and A. Zee, Phys. Rev. D **25**, 553 (1982); J. Maalampi, J.T. Peltoniemi, and M. Roos, PLB 220, 441(1989); J. Maalampi and M. Roos, Phys. Rept. **186**, 53 (1990); K. S. Babu, I. Gogoladze, P. Nath and R. M. Syed, Phys. Rev. D **72**, 095011 (2005) [hep-ph/0506312]; Phys. Rev. D **74**, 075004 (2006), [arXiv:hep-ph/0607244]; Phys. Rev. D **85**, 075002 (2012) [arXiv:1112.5387 [hep-ph]]; P. Nath and R. M. Syed, Phys. Rev. D **81**, 037701 (2010).

[9] K. S. Babu, I. Gogoladze, M. U. Rehman and Q. Shafi, Phys. Rev. D **78**, 055017 (2008) [arXiv:0807.3055 [hep-ph]].

[10] C. Liu, Phys. Rev. D **80**, 035004 (2009) [arXiv:0907.3011 [hep-ph]].

[11] S. P. Martin, Phys. Rev. D **81**, 035004 (2010) [arXiv:0910.2732 [hep-ph]].

[12] T. Ibrahim and P. Nath, Phys. Rev. D **84**, 015003 (2011) [arXiv:1104.3851 [hep-ph]].

[13] T. Ibrahim and P. Nath, Phys. Rev. D **82**, 055001 (2010) [arXiv:1007.0432 [hep-ph]].

[14] T. Ibrahim and P. Nath, Phys. Rev. D **81**, no. 3, 033007 (2010) [Erratum-ibid. D **89**, no. 11, 119902 (2014)] [arXiv:1001.0231 [hep-ph]].

[15] T. Ibrahim and P. Nath, Phys. Rev. D **78**, 075013 (2008) [arXiv:0806.3880 [hep-ph]].

[16] T. Ibrahim and P. Nath, Nucl. Phys. Proc. Suppl. **200-202**, 161 (2010) [arXiv:0910.1303 [hep-ph]].

[17] T. Ibrahim and P. Nath, Phys. Rev. D **87**, no. 1, 015030 (2013) [arXiv:1211.0622 [hep-ph]].

[18] T. Ibrahim, A. Itani and P. Nath, Phys. Rev. D **90**, no. 5, 055006 (2014).

[19] T. Ibrahim, A. Itani and P. Nath, arXiv:1503.01078 [hep-ph] (to appear in PRD).

[20] A. Aboubrahim, T. Ibrahim and P. Nath, Phys. Rev. D **89**, no. 9, 093016 (2014) [arXiv:1403.6448 [hep-ph]].

[21] A. Aboubrahim, T. Ibrahim, A. Itani and P. Nath, Phys. Rev. D **89**, no. 5, 055009 (2014) [arXiv:1312.2505 [hep-ph]].

[22] A. Aboubrahim, T. Ibrahim and P. Nath, Phys. Rev. D **88**, 013019 (2013) [arXiv:1306.2275 [hep-ph]].

[23] A. Aboubrahim, T. Ibrahim and P. Nath, Phys. Rev. D **91**, no. 9, 095017 (2015) [arXiv:1503.06850 [hep-ph]].

[24] J. Ellis, S. Ferrara, and D. V. Nanopoulos, Phys. Lett. **114B** (1982) 231; W. Buchmuller and D. Wyler, Phys. Lett. B121 (1983) 321; F. del'Aguila, M. B. Gavela, J. A. Grifols and A. Mendez, Phys. Lett. B126 (1983) 71; J. Polchinski and M. B. Wise, Phys. Lett. B125 (1983) 393; E. Franco and M. Mangano, Phys. Lett. B135 (1984) 445.

[25] P. Nath, Phys. Rev. Lett. **66**, 2565 (1991).

[26] T. Ibrahim and P. Nath, Phys. Lett. B **418**, 98 (1998) [hep-ph/9707409]; Phys. Rev. D **57**, 478 (1998) [hep-ph/9708456]; Phys. Rev. D **58**, 111301 (1998) [hep-ph/9807501]; Phys. Rev. D **61**, 093004 (2000) [hep-ph/9910553].

[27] T. Falk and K. A. Olive, Phys. Lett. B **439**, 71 (1998) [hep-ph/9806236]; M. Brhlik, G. J. Good and G. L. Kane, Phys. Rev. D **59**, 115004 (1999) [hep-ph/9810457].

[28] K. S. Babu, B. Dutta and R. N. Mohapatra, Phys. Rev. D **61**, 091701 (2000) [hep-ph/9905464].

[29] D. McKeen, M. Pospelov and A. Ritz, Phys. Rev. D **87**, no. 11, 113002 (2013) [arXiv:1303.1172 [hep-ph]].

[30] T. Moroi and M. Nagai, Phys. Lett. B **723**, 107 (2013) [arXiv:1303.0668 [hep-ph]].

[31] W. Altmannshofer, R. Harnik and J. Zupan, JHEP **1311**, 202 (2013) [arXiv:1308.3653 [hep-ph]].

[32] M. Dhuria and A. Misra, Phys. Rev. D **90**, no. 8, 085023 (2014) [arXiv:1308.3233 [hep-ph]].

[33] R. N. Mohapatra, Phys. Scripta **90**, no. 8, 088004 (2015) [arXiv:1503.06478 [hep-ph]].

[34] A. Manohar and H. Georgi, Nucl. Phys. B **234**, 189 (1984).

[35] C. A. Baker, D. D. Doyle, P. Geltenbort, K. Green, M. G. D. van der Grinten, P. G. Harris, P. Iaydjiev and S. N. Ivanov *et al.*, Phys. Rev. Lett. **97**, 131801 (2006) [hep-ex/0602020].

[36] T. M. Ito, J. Phys. Conf. Ser. **69**, 012037 (2007) [nucl-ex/0702024 [NUCL-EX]].

[37] Particle Data Group, Chin. Phys. C, 38, 090001 (2014)